Ketogenic diet therapy for pediatric epilepsy is associated with alterations in the human gut microbiome that confer seizure resistance in mice

Gregory R. Lum*[1], Sung Min Ha[1], Christine A. Olson[1], Montgomery Blencowe[1], Jorge Paramo[1], Beck Reyes[2], Joyce H. Matsumoto[2], Xia Yang[1], and Elaine Y. Hsiao*[1,3]

[1] Department of Integrative Biology & Physiology, University of California, Los Angeles, Los Angeles, CA 90095, USA

[2] Department of Pediatrics, Division of Pediatric Neurology, David Geffen School of Medicine, University of California, Los Angeles, CA 90095, USA

* Correspondence to: glum@g.ucla.edu, ehsiao@g.ucla.edu

[3] Lead Contact

SUMMARY

The gut microbiome modulates seizure susceptibility and the anti-seizure effects of the ketogenic diet (KD) in animal models, but whether these relationships translate to KD therapies for human drug-resistant epilepsy is unclear. Herein, we find that the clinical KD shifts the function of the gut microbiome in children with refractory epilepsy. Colonizing mice with KD-associated human gut microbes confers increased resistance to 6-Hz psychomotor seizures, as compared to colonization with gut microbes from matched pre-treatment controls. Parallel analysis of human donor and mouse recipient metagenomic and metabolomic profiles identifies subsets of shared functional features that are seen in response to KD treatment in humans and preserved upon transfer to mice fed a standard diet. These include enriched representation of microbial genes and metabolites related to anaplerosis, fatty acid beta-oxidation, and amino acid metabolism. Mice colonized with KD-associated human gut microbes further exhibit altered hippocampal and frontal cortical transcriptomic profiles relative to colonized pre-treatment controls, including differential expression of genes related to ATP synthesis, glutathione metabolism, oxidative phosphorylation, and translation. Integrative co-occurrence network analysis of the metagenomic, metabolomic, and brain transcriptomic datasets identifies features that are shared between human and mouse networks, and select microbial functional pathways and metabolites that are candidate primary drivers of hippocampal expression signatures related to epilepsy. Together, these findings reveal key microbial functions and biological pathways that are altered by clinical KD therapies for pediatric refractory epilepsy and further linked to microbiome-induced alterations in brain gene expression and seizure protection in mice.

42 ## INTRODUCTION

43

44 The low-carbohydrate, high-fat ketogenic diet (KD), is a mainstay treatment for refractory
45 epilepsy, particularly in children who do not respond to existing anti-epileptic drugs. The efficacy
46 of the KD is supported by multiple retrospective and prospective studies, which estimate that
47 ~30% of pediatric patients become seizure-free and ~60% experience substantial benefit with
48 >50% reduction in seizures (Coppola et al., 2002; Freeman et al., 1998; Hoon et al., 2005; Neal
49 et al., 2008). However, use of the KD for treating pharmacoresistant epilepsy remains low due to
50 difficulties with implementation, dietary compliance, and adverse side effects (Kossoff et al.,
51 2018). Even with successful seizure reduction, retention of epileptic children on the KD is a
52 reported 13% by the third year of dietary therapy (Hemingway et al., 2001). The primary reasons
53 cited for discontinuation include “diet restrictiveness” and “diet side effects,” in addition to low diet
54 responsiveness. While many pioneering studies have proposed important roles for
55 immunosuppression, ketone bodies, anaplerosis, and gamma-aminobutyric acid (GABA)
56 modulation in mediating the neuroprotective effects of the KD, they do not fully account for the
57 clinical heterogeneity in patient responsiveness. Exactly how the KD confers protection against
58 epilepsy in individuals with varied seizure semiologies remains unclear, and the biological
59 determinants of patient responsiveness to the KD are poorly understood.

60

61 The gut microbiome plays an integral role in mediating effects of diet on multiple aspects of host
62 physiology, including metabolism, neural activity, and behavior (Singh et al., 2017; Sonnenburg &
63 Bäckhed, 2016). To date, a few clinical studies have reported associations between the KD
64 regimens and alterations in the composition and/or functional potential of the gut microbiota in
65 epileptic individuals (Lindefeldt et al., 2019; G. Xie et al., 2017; Y. Zhang et al., 2018). While
66 promising, thus far there is little consistency across these different reports in the specific microbial

67 taxa or gene pathways that correlate with the KD. Moreover, functional consequences of the KD-
68 associated human epilepsy microbiome on host seizure susceptibility remain unknown. We
69 previously reported that KD-induced alterations in the gut microbiome were necessary and
70 sufficient for mediating the seizure protective effects of KD chow in two mouse models for
71 refractory epilepsy – the 6-Hz psychomotor seizure model and the *Kcna1* deficiency model for
72 sudden unexpected death in epilepsy (SUDEP) (Olson et al., 2018). Similarly, in a rat injury model
73 of infantile spasms, transfer of the KD-induced gut microbiota into naïve animals fed a control diet
74 reduced spasms (Mu et al., 2022). In addition, taxonomic differences in the gut microbiome were
75 correlated with seizure severity and seizure protection in response to KD chow in the *Scn1a*
76 deficiency model for Dravet syndrome (Miljanovic & Potschka, 2021). Together, these findings
77 across various seizure models provide proof-of-principle that the KD alters the gut microbiome in
78 ways that can promote seizure protection. However, whether these results from rodent studies
79 apply to human epilepsy, the human gut microbiome, and clinical KD regimens used to treat
80 pediatric epilepsy is still unknown, and the core microbial functions that impact seizure
81 susceptibility are unclear.
82
83 Herein, we perform a prospective study of KD interventions in children with refractory epilepsy
84 and test causal effects of the human gut microbiome before and after initiating clinical KD
85 regimens on seizure susceptibility in mice. We evaluate functional changes in the human gut
86 microbiome that are associated with KD treatment in pediatric epilepsy patients. We further
87 identify select features of the clinical KD-associated gut microbiome that are shared across both
88 human donors and inoculated mouse recipients that correlate with microbiome-dependent seizure
89 protection in mice. Finally, we identify key network interactions between the gut microbiome,
90 metabolites, and brain transcriptome that may contribute to the ability of the clinical KD-associated
91 human gut microbiome from pediatric epilepsy patients to promote seizure protection in mice.
92

93 ## RESULTS

94

95 ### Clinical KD regimens elicit shared functional features of the gut microbiome in a cohort
96 of children with refractory epilepsy

97

98 The KD is commonly prescribed for pediatric refractory epilepsy, wherein children consume
99 commercial ketogenic infant formula and/or fat-rich, carbohydrate-restricted meals with dietary
100 guidance from clinicians and registered dieticians (Kossoff et al., 2018). Notably, treatment
101 regimens for the KD vary from patient to patient. KD composition depends on patient tolerability,
102 which dictates the ratio of fat intake relative to carbohydrate and protein. Additionally, variable
103 food sources determine the specific macro- and micro-nutrients that comprise ketogenic meals.
104 Moreover, the KD is prescribed broadly for various forms of refractory epilepsy, the treatment
105 population varies in genetic risk, seizure semiology, and past anti-epileptic drug exposures,
106 among other factors. In order to assess effects of clinically-relevant KD treatments for refractory
107 epilepsy on the gut microbiome, we therefore conducted a prospective study of 10 children with
108 pediatric refractory epilepsy who were newly enrolled to the Ketogenic Diet Program at UCLA
109 Mattel Children's Hospital (**Table S1**). From each patient, we collected a stool sample within 1
110 day before initiating a KD regimen (pre-KD sample) and after approximately 1 month of adherence
111 to a clinically-guided KD (post-KD sample). 1 month was chosen as a time point at which we
112 expected to observe stabilized microbial responses to the dietary regimen (David et al., 2014).

113

114 Data from 16S rRNA gene amplicon sequencing of fecal samples indicated no significant
115 difference in bacterial α-diversity in the post-KD fecal microbiota from pediatric epilepsy patients
116 relative to their matched pre-KD internal controls (**Figure S1A, Table S2**). Principal coordinates
117 analysis of unweighted and weighted Unifrac distances revealed substantial variation across
118 individuals in baseline composition of the pre-KD microbiota (**Figure S1B**). Additionally, the

119 clinical KD elicited differential shifts in bacterial β-diversity and varied responses across post-KD
120 samples relative to their matching pre-KD controls, which were not significantly associated with
121 demographic or clinical measures, such as age, sex, and prior anti-epileptic drug exposure
122 (**Figure S1B**, Table S1, Yassour et al., 2016). Consistent with the inter-individual variation in
123 microbial taxonomic profiles, ANCOM and ANOVA analyses (paired or unpaired) identified no
124 significant differences in relative abundances in particular bacterial taxa when considering all
125 post-KD sample relative to their matched pre-KD controls (**Figures S1C)**. These results indicate
126 that, within this particular study cohort, there are no shared effects of the clinical KD on the
127 microbial composition of the gut microbiota of children with refractory epilepsy.
128
129 Functional redundancy is common across different microbial species of the human gut microbiota
130 (Tian et al., 2020). In light of the varied bacterial taxonomic profiles at baseline and in response
131 to dietary treatment, we next asked whether the clinical KD is associated with shared alterations
132 in the functional potential of the gut microbiota from children with pediatric epilepsy. Shotgun
133 metagenomic profiling and pathway analysis indicated that compared to pre-KD samples, post-
134 KD samples shared a significant decrease in relative abundance of genes belonging to the top 26
135 most abundant functional pathways, which together comprised >94% of the pathway diversity
136 detected (**Figure S1D and S1E, Table S3**). This corresponded with a significant increase in the
137 number of total observed pathways in post-KD samples compared to their respective pre-KD
138 controls (**Figure S1F**). These observations suggest that the clinical KD restricts the membership
139 of various types of microbial taxa that harbor genes related to prevalent functions and/or enriches
140 for microbial taxa that harbor genes related to previously rare or underrepresented functions. In
141 particular, post-KD samples exhibited significant enrichment of genes related to formaldehyde
142 assimilation, guanosine nucleotide degradation, and L-proline biosynthesis, and decreased
143 representation of genes related to aerobactin biosynthesis, as compared to pre-KD controls
144 (**Figure S1G, Discussion**). There were also modest increases in genes related to GDP-mannose

145 biosynthesis, 2-methylcitrate cycle, and glycol metabolism and degradation, and decreases in
146 genes related to polyamine biosynthesis and biotin biosynthesis, subsets of which will be
147 discussed in greater detail in the following sections (**Figure S1G)**. Taken together, these data
148 suggest that treatment with KD regimens that differ in KD ratio and specific nutritional composition
149 elicit broad shifts in the functional potential of the gut microbiome that are shared across children
150 with varied subtypes of refractory epilepsy.
151

152 Transferring the fecal microbiota from KD-treated pediatric epilepsy patients to mice
153 confers seizure resistance

154

155 Causal influences of the human microbiome can be effectively studied in gnotobiotic mice,
156 wherein transferring microbes in a clinical sample into microbiota-deficient mice is used to
157 recapitulate the taxonomic and functional diversity of the donor human microbiota. To evaluate
158 whether gut microbes associated with the clinical KD impact seizure susceptibility, we inoculated
159 individual cohorts of germ-free (GF) mice with matched pre-KD and post-KD stool samples
160 collected from children with refractory epilepsy and maintained the colonized mice on standard
161 (non-ketogenic) mouse chow (control diet, CD). Each human donor sample (pre-KD and post-KD
162 from 10 individuals, as biological replicates) was inoculated into 14-16 GF mice (as technical
163 replicates) to enable cohort-level testing of susceptibility to 6-Hz psychomotor seizures (**Figure**
164 **1A**). The 6-Hz seizure model involves low-frequency corneal stimulation to induce acute complex
165 partial seizures reminiscent of human limbic epilepsy (Barton et al., 2001). Consistent with
166 refractory epilepsy, the 6-Hz model is resistant to several anti-epileptic drugs, but treatment with
167 KD chow effectively protects against 6-Hz seizures in rodents (Hartman et al., 2008), raising the
168 intensity of current required to elicit a seizure in 50% of the subjects tested (CC50, seizure
169 threshold). The 4-day time point was chosen as the maximum duration of time that a KD-induced
170 microbiota could be maintained in mice fed CD (Olson et al., 2018).

171

172 Despite the variation in bacterial diversity across patient gut microbiota (**Figure S1**), we observed
173 that GF mice colonized with microbes from the post-KD microbiota required greater intensity of
174 current to induce 6-Hz seizures (**Figure 1B, Table S4**) as compared to controls colonized with
175 microbes from the pre-KD microbiota. This effect was seen when comparing post-KD vs. pre-KD
176 microbiota transfer for individual technical replicates per patient (**Figure 1B)**, as well as when
177 data were averaged across all patients (**Figures 1C and 1D**). In addition, compared to pre-KD
178 controls, mice colonized with microbes from the post-KD microbiota required increased intensity
179 of current to elicit one or more recurred seizures observed after the initial stimulus-induced seizure
180 (**Figure 1E**), indicating that transfer of the post-KD human microbiota promotes resistance to both
181 primary induced seizures and remission seizures in mice. On average, the post-KD samples
182 raised seizure thresholds by 21.0% $\pm$ 6.7% relative to matched pre-KD controls (**Figures 1C and**
183 **1D**). This aligns with both our previously published data on the average effect size of KD chow on
184 wildtype mice tested in the 6-Hz seizure assay (21.9%, Olson et al., 2018), and the observed
185 24.0% increase in seizure threshold seen in GF mice colonized with a conventional adult mouse
186 microbiota (GF-conv) and fed a 6:1 KD chow, as compared to conventionalized controls fed a
187 standard vitamin- and mineral-matched control diet (**Figure 1B**). Discrepancies in effect size
188 across patient samples were largely driven by differences between responses for pre-KD controls
189 (**Figure 1B**), suggesting that the comparatively low microbial diversity resulting from cross-host
190 species transfer increases seizure susceptibility. Consistent with this, we previously observed that
191 decreasing microbial diversity via antibiotic treatment reduced seizure threshold in the 6-Hz assay
192 (Olson et al., 2018). Overall, these results indicate that inoculating mice with the clinical KD-
193 associated human gut microbiota increases 6-Hz seizure threshold to levels similar to the effect
194 sizes seen with direct consumption of the experimental 6:1 KD.

195

196 Human microbiota transplantation to mice involves oral inoculation with a human stool
197 suspension, which is comprised of microbial biomass, as well as undigested food matter and
198 secreted molecules from the host and microbiota. As such, effects seen in response to the transfer
199 procedure could be due to the KD-associated gut microbiota or microbiota-independent dietary
200 or host factors. To gain insight into whether bacteria from the gut microbiota are required for
201 mediating the increases in seizure protection seen with inoculation of the human post-KD
202 microbiota into mice, mice inoculated with a randomly selected post-KD donor sample were
203 treated with broad-spectrum antibiotics (**Abx**) to deplete the microbiota, or with vehicle (**Veh**) as
204 negative control (**Figures S2A and S2B**). Mice that were inoculated with the post-KD sample and
205 treated with Veh displayed seizure thresholds that were comparable to that seen previously in
206 recipient mice without the added Veh treatment (**Figures S2C, S2D, and 1B and Table S4**). This
207 suggests that the post-KD sample induced increases in seizure resistance that were maintained
208 for at least 12 days in mice fed CD. In contrast, depletion of gut bacteria in mice that were
209 colonized with the post-KD microbiota decreased seizure thresholds to levels that were lower than
210 previously seen in pre-KD colonized controls (**Figures S2C, S2D, and 1B**). These results indicate
211 that bacterial members of the post-KD microbiota are necessary for mediating the increases in
212 seizure threshold seen in response to transfer of the clinical-KD associated microbiota from a
213 pediatric epilepsy patient into mice.
214
215 Administration of microbial metabolites or other microbiome-dependent molecules, in lieu of viable
216 microbiota, has been reported to ameliorate symptoms of recurrent *Clostridiodes difficile* infection,
217 inflammatory bowel disease, and multiple sclerosis, among other conditions (Cekanaviciute et al.,
218 2017; Levy et al., 2015; Ott et al., 2017). To gain insight into whether administration of clinical
219 KD-associated intestinal small molecules is sufficient to confer seizure protection in mice, a post-
220 KD donor sample selected at random was sterile filtered and then administered to a cohort of GF
221 recipient mice (**Figure S3A**), alongside controls that were administered the unfiltered post-KD

222 suspension, as was done previously for human microbiota inoculation (**Figures S3A and 1B**). At
223 4 days post inoculation, mice that were treated with the post-KD filtrate exhibited lower seizure
224 threshold compared to controls that were treated with the corresponding unfiltered post-KD
225 suspension (**Figures S3B and S3C and Table S4**). These data indicate that clinical KD-
226 associated small molecules in the post-KD fecal sample from a pediatric epilepsy patient are not
227 sufficient to confer persistent seizure protection in mice.
228
229 Orally administered microbial metabolites can be rapidly absorbed and cleared from systemic
230 circulation within a few hours of administration (Abrams & Bishop, 1967; Williams et al., 2020).
231 To further assess whether clinical KD-associated intestinal small molecules, including microbial
232 metabolites, acutely modulate seizure susceptibility, mice were orally gavaged with a sterile-
233 filtered post-KD sample and assessed 2 hours later for 6-Hz seizure threshold, rather than 4 days
234 later as in the previous experiments (**Figure S4A**). Mice treated with post-KD filtrate exhibited
235 significantly increased seizure protection compared to controls treated with pre-KD filtrate
236 (**Figures S4B and S4C and Table S4**), with seizure thresholds that approached those seen after
237 inoculation of the post-KD suspension (**Figures S4B and 1B**). These data indicate that
238 administration of clinical KD-associated intestinal small molecules can acutely confer seizure
239 protection in mice over short timescales (i.e., 2 hours, **Figure S4**), which diminishes by 4 days
240 post treatment (**Figure S3**). Taken together, the results presented in these series of experiments
241 suggest that the clinical KD for pediatric refractory epilepsy is associated with alterations in
242 metabolic activities of the gut microbiota that promote seizure resistance in mice.
243
244 While the “humanization” of mice with microbiota from clinical stool samples is a powerful tool for
245 translational microbiome research (Turnbaugh et al., 2009), the approach has technical and
246 biological limitations that warrant careful consideration (Walter et al., 2020). Namely, while much
247 of the taxonomic and functional diversity of the donor inoculum can be recapitulated in recipient

248 mice (Bokoliya et al., 2021), developmental influences and host-specific selection (Rawls et al.,
249 2006), among other factors, preclude full “engraftment” of the human gut microbiota in GF mice
250 (Walter et al., 2020). To evaluate the fidelity of fecal microbiota “transplantation” from pediatric
251 epilepsy patients to GF mice, we subjected both the donor pre-KD and post-KD stool samples
252 and corresponding recipient mouse fecal pellets collected at 4 days post-inoculation (the day of
253 seizure testing) to 16S rRNA gene amplicon sequencing (**Figure 1A, Tables S2 and S5**).
254 Principal coordinates analysis of bacterial taxonomic data revealed overt clustering of donor
255 samples with matched recipient samples only for select patients, while the remaining exhibited
256 substantial variation and no noticeable clustering (**Figure S5A**). There was no significant
257 difference in α-diversity between pre-KD and post-KD fecal microbiota for either donor or recipient
258 samples (**Figures S5B**). However, we observed a significant reduction in α-diversity, with an
259 average decrease of 38% for all mouse recipient microbiota relative to all human donor microbiota
260 (**Figure S5C**), indicating incomplete transfer or engraftment of the human microbiota in mice.
261 These results align with several previous reports of reduced bacterial α-diversity in mice
262 inoculated with human microbiota, with estimated decreases of 35%, 38%, and 50% (Blanton et
263 al., 2016; Sharon et al., 2019; Staley et al., 2017), suggesting that we achieved levels of transfer
264 fidelity that are consistent with those in the field. However, the inability to fully recapitulate the
265 taxonomic diversity of the human gut microbiota from pediatric epilepsy patients in mice draws
266 into question whether the increases in seizure resistance seen in mice inoculated with post-KD
267 microbiota are relevant to the actual clinical condition. We therefore focused subsequent
268 experiments on identifying and evaluating the subset of functional features of the KD-associated
269 human gut microbiome that are recapitulated in recipient mice, and the microbiome-dependent
270 alterations in host physiology that correspond with seizure protection in mice.
271

272 **Select functional features of the clinical KD-associated human microbiome are**
273 **recapitulated in colonized recipient mice and correlate with seizure protection**

274

275 Given the widespread use of the clinical KD for treating epilepsy, and an increasing number of
276 other neurodevelopmental and neurodegenerative disorders, elucidating how the activity of the
277 gut microbiome is altered by the clinical KD could reveal important insights into its physiological
278 effects. To identify microbiome associations with the clinical KD and further determine which of
279 the associations, if any, may modify seizure risk, we functionally characterized the gut microbiome
280 from pediatric epilepsy patients before and after treatment with the clinical KD, as well as from
281 gnotobiotic mice that were inoculated with the patient samples, and tested for causal outcomes
282 on seizure susceptibility. Metagenomic sequencing and analysis revealed microbial gene
283 pathways that were differentially abundant in post-KD samples relative pre-KD controls, and
284 shared between both human donor samples and mouse recipient samples (**Figure 2A, Tables**
285 **S3 and S6**). In particular, microbial genes relevant to fatty acid β-oxidation, glycol metabolism
286 and degradation, methylcitrate cycle I, methylcitrate cycle II, and proline biosynthesis were
287 similarly elevated in post-KD human samples and post-KD-inoculated mice compared to their
288 respective pre-KD controls (**Figures 2A and 2B**). These findings align with reported influences of
289 the KD on fatty acid oxidation (A. R. Kennedy et al., 2007), of carbohydrate restriction on
290 promoting the glyoxylate cycle (Puckett et al., 2017), and of fatty acid β-oxidation on the initiation
291 of the methylcitrate cycle (Clark & Cronan, 2005). Proline metabolism involves reactions with
292 glutamine, glutamate, ornithine, and arginine, which might relate to reported effects of KD on
293 amino acid metabolism, particularly of glutamine and glutamate (Yudkoff et al., 2007). In addition,
294 both post-KD human donor and mouse recipient samples exhibited reductions in microbial genes
295 relevant to polyamine biosynthesis and aerobactin biosynthesis (**Figures 2A and 2B**). The main
296 role of polyamine biosynthesis is generation of putrescine, mainly using the glucogenic amino
297 acid L-arginine which is consumer in reduced amounts while on the KD. Aerobactin, a sidophore,
298 biosynthesis uses the ketogenic amino acid L-lysine, which is also essential for acetyl-CoA
299 synthesis and energy production during ketosis. These data suggest that the consumption of a

300 clinical KD by children with refractory epilepsy enriches for gut microbes that have the functional
301 capacity to metabolize dietary fats and to perform anaplerotic reactions when dietary
302 carbohydrates are restricted. The findings further indicate that these general features of the KD-
303 associated human gut microbiome are phenocopied in recipient mice that exhibit microbiome-
304 dependent protection against 6-Hz seizures.
305
306 The observed metagenomic signatures reveal clinical KD-associated changes in the functional
307 potential of the gut microbiome that are preserved upon transfer to GF mice. To identify clinical
308 KD-induced alterations in the functional activity of the gut microbiome, we performed untargeted
309 metabolomic profiling of aliquots of the same donor fecal samples from pediatric epilepsy patients
310 collected before and after initiating the KD regimen, and of both fecal and serum samples from
311 recipient mice that were inoculated with the pre-KD or post-KD human fecal microbiota and fed
312 CD (**Tables S7, S8, and S9**). Results from clinical laboratory testing of human blood samples
313 confirmed that the month-long clinical KD regimen elevated serum β-hydroxybutyrate (**BHBA**)
314 levels and reduced serum glucose levels, relative to pre-KD concentrations, in pediatric refractory
315 epilepsy patients (**Figure 2C**). Decreases in glucose, but not BHBA, were similarly seen in human
316 post-KD stool samples relative to matched pre-KD controls (**Figure 2C**), which is consistent with
317 dietary carbohydrate restriction and KD-induced BHBA synthesis by the liver to elevate systemic,
318 but not fecal, BHBA levels (Westman et al., 2007). Transfer of the post-KD human microbiota into
319 mice yielded no significant differences in serum BHBA or glucose relative to pre-KD recipient
320 controls (**Figure 2C**), indicating that the clinical KD-associated microbiota does not sufficiently
321 promote key systemic features of ketosis in mice fed the standard CD. Notably, however, mice
322 that were inoculated with post-KD human microbiota and fed CD exhibited statistically significant
323 increases in fecal BHBA levels relative to matched pre-KD recipient controls (**Figure 2C**). This
324 could reflect alterations in intestinal synthesis of BHBA (Mierziak et al., 2021) and/or in microbial
325 utilization of host-derived BHBA (Ang et al., 2020). Since this effect was not seen in the donor

326 human fecal samples, we reasoned that this phenotype is likely an artifact of the “transplantation”
327 approach and/or experimental design, and therefore not relevant to the clinical condition. These
328 results suggest that transfer of the clinical KD-associated human gut microbiota into mice
329 promotes resistance to 6-Hz seizures (**Figure 1**) through mechanisms that act independently of
330 ketosis.
331
332 We further assessed results from untargeted metabolomic profiling to identify metabolites that
333 were differentially abundant in post-KD samples relative to pre-KD controls and patterns that were
334 shared across human donor and mouse recipient samples (**Figure 2D, Figure S6, Tables S7**
335 **and S8)**. Despite heterogeneity in the patient population and specific clinical KD regimens, 79
336 metabolites were significantly differentially abundant in fecal samples from post-KD human fecal
337 samples relative to their matched pre-KD controls (**Figure S6A, Table S7**). 336 metabolites were
338 identified in both the human fecal samples and mice fed the 6:1 KD chow vs. vitamin- and mineral-
339 matched control chow for 2 weeks samples, previously published by our group (**Table S10,** Olson
340 et al., 2018). 35 metabolites were differentially regulated in human fecal samples and 169
341 metabolites were differentially regulated in mouse fecal samples (**Figure S6B**). Of these
342 significantly altered metabolites, 20 were found to be changed in the same direction across human
343 and mouse samples (**Figure S6B and S6C**). These included KD-induced increases in levels of
344 metabolites related to fatty acid beta-oxidation, such as palmitoleoylcarnitine (C16:1) and
345 oleoylcarnitine (C18:1), and a decrease in kynurenine which have previously been associated
346 with seizure susceptibility (Żarnowska et al., 2019). This statistically significant overlap suggests
347 that there are biochemical changes that are shared across clinical KD treatments for pediatric
348 epilepsy and mouse models of KD, and that some of the fecal metabolomic alterations observed
349 in KD-treated epilepsy patients are a direct consequence (rather than correlate) of dietary
350 intervention. Of the 26 significantly differentially abundant metabolites shared in human and
351 mouse, 21 (~81%) were further significantly altered by antibiotic treatment to deplete gut bacteria

352 in KD-fed mice (**Figure S6B,** Olson et al., 2018). Taken together, these data indicate that clinical
353 KD regimens alter fecal metabolites in children with refractory epilepsy, a subset of which have
354 the potential to be microbiome-dependent.
355
356 Although there was substantial variability in taxonomic composition of microbiota within mouse
357 recipients of the same experimental condition (**Figure S1-S2**), fecal samples from mouse
358 recipient cohorts exhibited statistically significant alterations in 45 metabolites that were shared
359 when considering all post-KD mouse recipient fecal samples relative to their pre-KD controls
360 (**Table S8, Figure S6A**). Notably, however, none of these 45 differentially abundant metabolites
361 in mouse feces were identical to the 79 differentially abundant metabolites seen in human donor
362 fecal samples (**Figure S6A**), which could reflect host specific metabolite utilization and the fact
363 that recipient mice were fed standard chow (CD), while human donors were consuming a clinical
364 KD at the time of sample collection. To gain insight into whether the differentially abundant
365 metabolites relate to similar biological functions, we performed metabolite set enrichment analysis
366 (MSEA) of the significantly altered metabolites in human vs. mouse (Pang et al., 2021). MSEA of
367 the significantly altered metabolites identified select chemical classes (**Figure 2D**) and metabolic
368 pathways (**Figure 2E**) that were similarly enriched in both human donor and mouse recipient post-
369 KD samples relative to pre-KD controls. In particular, there was shared enrichment of amino acid,
370 hydroxy fatty acid, sugar acid, phenylpropanoic acid, and monosaccharide-related metabolites
371 across post-KD conditions for both human donors and mouse recipients (**Figure 2D**). Differentially
372 abundant metabolites from human post-KD fecal samples also exhibited enrichment of bile acids
373 and other fatty acid derivatives (**Figure 2D, left**), which might reflect KD- and/or microbiome-
374 driven alterations in lipid metabolism (Joyce et al., 2014).
375
376 For metabolic pathways, post-KD samples for both human donor and mouse recipient conditions
377 exhibited differential abundance of metabolites related to methionine metabolism, glycine and

378 serine metabolism, and betaine metabolism (**Figure 2E**). While the biological relevance to KD is
379 unclear, one possibility is that these pathways reflect known influences of the KD on one-carbon
380 (1C) metabolism, a series of interlinking metabolic pathways that control levels of methionine,
381 serine, and glycine, and that integrate nutrient availability with cellular nutritional status (Ducker
382 & Rabinowitz, 2017). In addition, differentially abundant fecal metabolites from mouse post-KD
383 recipients mapped to pathways related to alpha linolenic acid and linoleic acid metabolism, fatty
384 acid biosynthesis, and beta-oxidation of very long chain fatty acids (**Figure 2E, right**), which
385 aligns with the observed metagenomic enrichment in microbial genes related to fatty acid
386 metabolism in response to the clinical KD (**Figure 2A-B**). Some of the differential metabolite
387 chemical subclasses and metabolic pathways in mouse fecal samples were similarly seen in
388 matched mouse serum samples (**Table S9**) – in particular, metabolites representing amino acid,
389 hydroxy fatty acid, and unsaturated fatty acid subclasses, and related to alpha linolenic acid and
390 linoleic acid metabolism, betaine metabolism, and beta-oxidation of fatty acids were altered in
391 both feces and serum of mice receiving post-KD samples relative to pre-KD controls (**Figure**
392 **S6D**). Taken together, these results suggest that the clinical KD induces alterations in the function
393 of the gut microbiome of pediatric epilepsy patients, and that a subset of these functional
394 characteristics may be phenocopied upon microbial transfer to mice, which develop microbiome-
395 dependent resistance to 6-Hz seizures.
396

397 **Transferring the fecal microbiota from KD-treated pediatric epilepsy patients to mice**
398 **induces alterations in brain gene expression**
399

400 Seizures result from atypical neural function related to discharge of electrical signals or failure to
401 constrain the spread of these signals. To gain insight into how colonization with microbes derived
402 from the fecal microbiota of KD-treated individuals may alter brain function to modify seizure
403 susceptibility, we performed transcriptomic profiling of brain tissues from cohorts of mice

404 colonized with microbes from the post-KD human microbiota or pre-KD controls. We focused on
405 the hippocampus and frontal cortex based on their relevance to human epilepsy, their involvement
406 in initiating psychomotor seizures in the 6-Hz seizure assay, and evidence that the microbiome
407 can alter gene expression and metabolites in these brain regions (Chauhan et al., 2022; Suarez
408 et al., 2018). RNA sequencing of hippocampal tissues revealed many differentially expressed
409 genes that were seen in post-KD samples relative to pre-KD controls (**Table S11**), including those
410 related to core cell biological processes relating to RNA processing, translation, cellular stress
411 response, TORC1 signaling, regulation of long-term synaptic potentiation, neuronal development,
412 and response to nutrient levels (**Figure 3A**). The most drastic alterations included upregulation of
413 *Dusp12, Bmpr1b,* and *Cmya5* and downregulation of *Abcc9*, *Ufsp1*, and *Tbx2* transcripts (**Figure**
414 **3B**). *Dusp12* is a dual specificity phosphatase that can dephosphorylate phosphothreonine and
415 phosphoserine (Muda et al., 1999)*, Bmpr1b,* a member of the bone morphogenic receptor family,
416 is a serine/threonine kinase influencing neuronal cell fate (Venugopal et al., 2012), and *Cmya5*
417 encodes for myospyrn which is essential for structural integrity during neuritogenesis (Hsiung et
418 al., 2019). *Abcc9* is an ATP-binding cassette transporter encoding the sulfonylurea receptor 2
419 subunit for potassium channels (Nelson et al., 2015), *Ufsp1* is a Ufm1 specific protease that
420 regulates ubiquitin-like conjugation and has been linked to seizures (Millrine et al., 2022), and
421 *Tbx2* is a transcription factor linked to neuronal cell cycle control and neuroinflammation
422 (Reinhardt et al., 2019). STRING network analysis additionally revealed top protein interaction
423 clusters enriched for essential biological processes including RNA processing, oxidative
424 phosphorylation, and cell cycle regulation, consistent with results from GO enrichment analysis
425 (**Figure 3A, 3C, 3D**), as well as endocytosis and glutathione metabolism (**Figure 3D**).
426
427 Some differentially expressed genes were also identified in frontal cortical tissues of post-KD
428 recipients relative to pre-KD controls (**Table S12**), which similarly to hippocampus, included those
429 related to core cell biological processes for RNA surveillance and catabolism, cellular stress

430 responses, TORC1 signaling, and further included genes related to potassium ion transport, and
431 core carbohydrate metabolism (**Figure S7A**). The most drastic alterations included upregulation
432 of *Serpinb1a, Nqo1,* and *Slc6a12* transcripts, and downregulation of *Aldh3b1, Setmar*, and *Tfb1m*
433 transcripts (**Figure S7B**). *Serpinb1a* is a serine/cysteine protease inhibitor (Huasong et al., 2015),
434 *Nqo1* encodes an antioxidant enzyme that primarily catalyzes the reduction of quinones (Ross &
435 Siegel, 2021), and *Slc6a12* encodes for a betaine-GABA transporter (Zhou et al., 2012). *Aldh3b1*
436 is an aldehyde dehydrogenase linked to oxidative stress reduction (Marchitti et al., 2007), *Setmar*
437 encodes a histone-lysine N-methyltransferase (Cordaux et al., 2006), and *Tfb1m* has been shown
438 to function as methyltransferase (Metodiev et al., 2009). STRING network clustering analysis
439 additionally revealed top protein interaction clusters enriched for transcription regulation,
440 translation, and oxidative phosphorylation, also seen in frontal cortex GO enrichment analysis
441 and in the hippocampal STRING network, as well as clusters enriched for calcium signaling,
442 transcriptional regulation, and translation (**Figure S7C, S7D**). Differentially expressed gene sets
443 from both hippocampus and frontal cortex were enriched for TORC1 signaling, cellular response
444 to stress, and oxidate phosphorylation through GO enrichment and STRING clustering, which
445 have all been shown to affect seizure susceptibility (Chan, 2001; Nguyen & Bordey, 2021). The
446 similarities between transcriptomic results from hippocampus and frontal cortex suggest that
447 colonization with post-KD microbes elicits key alterations in host metabolism that impact core
448 biological processes that are generally consistent across different brain regions. Overall, these
449 results indicate that mice that acquire seizure resistance in response to colonization with microbes
450 from the post-KD human gut microbiota exhibit alterations in hippocampal and frontal cortical
451 gene expression, relative to pre-KD recipient controls.
452
453 **Multi'omics analysis reveals network connections linking microbial genomic pathways**
454 **and metabolites to hippocampal transcripts related to epilepsy**
455

456 To further identify key gut microbial functions that may drive particular brain gene expression
457 signatures, we utilized microbe-metabolite vectors (MMVEC) (Morton et al., 2019) to build an
458 integrated network of fecal metagenomic, fecal metabolomic, serum metabolomic, hippocampal
459 transcriptomic, and frontal cortical transcriptomic datasets from mice inoculated with the human
460 pre-KD or post-KD microbiota (**Table S13**). We generated a parallel network comprised of fecal
461 metagenomic and fecal metabolomic datasets from human pre-KD and post-KD donor stool
462 samples to identify features similarly underscored in both human and mouse networks,
463 suggesting their clinical relevance. The human donor and mouse recipient networks were linked
464 by 3 common nodes - metagenomic pathways describing branched chain amino acid (BCAA)
465 biosynthesis (BRANCHED-CHAIN-AA-SYN-PWY), L-alanine fermentation (PROPFERM-PWY),
466 and co-enzyme A biosynthesis (COA-PWY), as well as pathways for arginine synthesis
467 (ARGSYN-PWY In the human network and ARGSYNSUB-PWY in the mouse network) (**Figure**
468 **4A,** center gray and green nodes). The shared BCAA biosynthesis, co-enzyme A biosynthesis,
469 and arginine synthesis pathways were also identified by weighted key driver analysis as highly
470 interconnected across the 'omics datasets and essential regulator nodes of the network (Ding et
471 al., 2021) (**Figure 4A**, diamonds). The human donor network also contained an additional key
472 driver metagenomic node for isoleucine biosynthesis (ILEUSYN-PWY), which aligns with the
473 metagenomic node for BCAA biosynthesis. Consistent with the shared metagenomic key drivers
474 between mouse and human networks, the human fecal metabolomic module was enriched for
475 nodes related to valine, leucine, and isoleucine (BCAA) and CoA biosynthesis (**Figure 4A**, gray
476 diamond node). In the mouse network, metabolomic modules included nodes related to
477 glycerophospholipid metabolism for fecal metabolites and pentose and glucuronate
478 interconversions for serum metabolites (**Figure 4A,** orange and sea green nodes). Nodes for fecal
479 1-(1-enyl-palmitoyl)-2-linoleoyl-GPC (P-16:0/18:2)*, 1-(1-enyl-palmitoyl)-2-palmitoyl-GPC (P-
480 16:0/16:0)*, 1-(1-enyl-palmitoyl)-2-arachidonoyl-GPC (P-16:0/20:4)*, 3-hydroxybutyrate (BHBA),
481 and myo-inositol (**Figure 4A**, orange metabolite nodes in red font) were similarly identified as

482 differentially abundant in individual metabolomic analyses for recipient post-KD fecal samples
483 relative to pre-KD controls (**Table S7**). These mouse metagenomic and metabolomic modules
484 were linked to 5 transcriptomic modules for hippocampal genes and 3 for frontal cortical genes
485 (**Figure 4A,** bottom section). The hippocampal transcript modules were enriched for nodes related
486 to regulation of telomerase RNA localization to Cajal body, glycosylphosphatidylinositol (GPI)
487 anchor biosynthetic processes, Wnt signaling, and neuron generation and migration (**Figure 4A**).
488 The frontal cortical transcript modules were enriched for nodes related to regulation of catabolic
489 processes, lipase activity, and BCAA transmembrane transporter activity (**Figure 4A**). This
490 suggests that these particular biological processes are most closely associated with the microbial
491 functional features identified in the network. The transcript nodes included 41 hippocampal genes
492 and 4 frontal cortical genes that were similarly identified in individual transcriptomic analyses as
493 differentially expressed in post-KD recipient mice relative to pre-KD controls (**Figure 4A**, transcript
494 nodes in red font). The higher number of connections between metabolomic modules and
495 hippocampal transcripts suggests that the gut microbiome may exhibit a greater regulatory role
496 for the hippocampus than for the frontal cortex in post-KD recipient mice compared to pre-KD
497 controls. Of particular interest are the links between fecal metabolites related to
498 glycerophospholipid metabolism, which are regulated by the microbiome (Zheng et al., 2021), and
499 hippocampal transcript modules enriched for Wnt signaling and GPI anchor biosynthetic
500 processes, pathways implicated in seizure susceptibility (Hodges & Lugo, 2018; Wu et al., 2020).
501
502 To gain insight into whether the hippocampal and frontal cortical transcripts that co-occur with
503 microbial metagenomic and metabolomic features have been implicated in human epilepsy, single
504 nucleotide polymorphisms (SNPs) identified from epilepsy genome-wide association studies
505 (GWAS) were mapped to genes using hippocampus and frontal cortex splicing quantitative trait
506 loci (sQTLs) and expression quantitative trait loci (eQTLs) to represent epilepsy-associated genes
507 informed by GWAS. The mouse orthologs of these human GWAS disease genes were then

508 compared with hippocampal and frontal cortical transcriptomic results to identify DEGs in post-
509 KD vs pre-KD recipients that have been implicated in genetic risk for human epilepsy. There was
510 a statistically significant enrichment of the hippocampal DEGs in the epilepsy GWAS (p=0.003),
511 but no significant enrichment of the frontal cortical DEGs in the epilepsy GWAS (p=0.26) (**Figure**
512 **4B**). These results suggest that microbial alterations in hippocampal gene expression may
513 contribute to the microbiome-dependent increases in seizure resistance seen in post-KD recipient
514 mice compared to pre-KD controls. From the co-occurrence network, 5 hippocampal DEGs were
515 linked to epilepsy GWAS results: *Atp5c*, which encodes mitochondrial ATP synthase; *Rprd2,*
516 which encodes a transcriptional repressor that modulates RNA polymerase II activity; *Gnaz*, which
517 encodes G protein alpha subunit that regulates ion equilibrium and chaperone-mediated folding;
518 *Cfdp1*, which encodes a subunit of the chromatin remodeling complex and is important for cell
519 division, and *Mro*, which encodes a nucleolus protein proposed to be testis-determining in the
520 reproductive tract, but expressed in the nervous system with as yet unknown function. Overall,
521 the multi'omics analysis of human donor and mouse recipient datasets together with epilepsy
522 GWAS mapping to hippocampal and frontal cortical DEGs identified key microbial genomic
523 pathways and microbially modulated metabolites that may contribute to alterations in the
524 expression of particular hippocampal genes in mice that exhibit microbiome-induced protection
525 against 6-Hz seizures.
526
527 **DISCUSSION**
528
529 Results from this research provide evidence from a treatment study of children with refractory
530 epilepsy, coupled with functional testing in gnotobiotic mice, that clinical KD regimens alter the
531 function of the gut microbiome in ways that could contribute to seizure protection. We assessed
532 microbiome composition and function in 10 children with refractory epilepsy shortly before
533 initiating and approximately one month after adherence to classical KD regimens. Following

534 clinical practice, the patient cohort was heterogeneous in type and underlying cause of refractory
535 epilepsy, as well as the ratio of fat to carbohydrate and protein and specific nutritional composition
536 of the KD they consumed (**Table S1**). This highlights the diversity of epilepsies that resist current
537 antiepileptic drugs and the broad range of KD interventions that are administered to treat pediatric
538 refractory epilepsy. Consistent with this heterogeneity, we observed that participants varied
539 substantially in the composition of the fecal microbiota at baseline and in response to KD
540 treatment. There was no clear KD-induced taxonomic signature of the gut microbiota that was
541 shared across the study population, which contrasts prior studies of KD treatments for epilepsy
542 that each reported alterations in the gut microbiota in response to a KD. Our results, however,
543 support the finding that little to no consistency in specific microbial taxa affected exists across
544 studies (Özcan et al., 2022).
545
546 Despite variation in microbiota composition, we observed evidence of shared functional features
547 of the gut microbiome that were seen with KD treatment across participants in the study. This
548 aligns with the notion of functional redundancy of gut microbes, wherein phylogenetically
549 unrelated species can exhibit the same genetically-encoded biological activities (Tian et al.,
550 2020). Results from metagenomic sequencing indicated that microbial genes related to fatty acid
551 β-oxidation, 2-methylcitrate cycle, glycol metabolism, and proline biosynthesis were more highly
552 represented in the gut microbiota of epileptic children after treatment with the KD compared to
553 their internal pre-treatment controls. β-oxidation by select microbes in anaerobic environments
554 enables them to utilize fatty acids from the diet as energy sources, wherein saturated and
555 unsaturated fatty acids are oxidized into acetyl-CoA (Yao & Rock, 2017). β-oxidation of dietary
556 odd-chain fatty acids additionally produces propionyl-CoA, which can be toxic to cells, so the
557 methylcitrate cycle enables microbes to further catabolize propionyl-CoA into pyruvate and
558 succinate (Dolan et al., 2018). Glycol, including glycolate and glyoxylate, metabolism allows
559 microbes to use products from fatty acid oxidation to fuel gluconeogenesis (Ahn et al., 2016).

560 Proline synthesis from the central metabolite glutamate, via intermediates amino acids arginine
561 and ornithine, is widely upregulated in bacteria to counteract growth in osmotically unfavorable
562 conditions (Stecker et al., 2022). The elevated representation of genes related to these pathways
563 in the post-KD samples suggests that the clinical KD shapes the gut microbiome to enrich
564 microbial taxa that digest fat and synthesize carbohydrates under fat-rich, carbohydrate-limited
565 conditions. These metagenomic features of the human microbiome from pediatric epilepsy
566 patients consuming a clinical KD were preserved upon transfer to GF mice that were fed a
567 standard diet, suggesting that the source microbes are maintained under non-ketogenic dietary
568 conditions.
569
570 Aligning with results from metagenomic sequencing, metabolomic profiling of fecal samples from
571 KD-treated epileptic children revealed statistically significant alterations in several metabolites,
572 including subsets of amino acids, sugar acids, hydroxy fatty acids, bile acids, and other fatty acid
573 derivatives, which reflect KD-, and potentially microbiome-, induced alterations in lipid and amino
574 acid metabolism. In particular, glutamate and ornithine, both precursors of proline, were
575 significantly decreased in post-KD human samples, relative to pre-KD controls, which may align
576 with the observed metagenomic alterations in proline biosynthesis pathways. These metabolite
577 alterations were induced by KD consumption in mice, and modified by microbiota depletion in
578 mice, suggesting a causal response to the clinical KD in the human cohort that is dependent on
579 the gut microbiome. Microbially modulated increases in palmitoleoylcarnitine (C16:1) were also
580 seen in KD-fed mice and in post-KD human samples, alongside several other lipid species,
581 aligning with the high fat content of the KD and roles for the gut microbiome in lipid metabolism
582 (Joyce et al., 2014).
583
584 The individual metabolite changes seen in human donors, including those induced by KD in a
585 microbiome-dependent manner, were not specifically recapitulated by microbiome transfer to GF

586 mice that were fed standard chow. This is perhaps not surprising given the important role of
587 dietary composition in driving microbial activity (David et al., 2014). While no specific metabolite
588 shifts were shared, a few pathway-level metabolomic changes were consistent between post-KD
589 fecal samples from human donor (consuming the clinical KD) and mouse recipients (fed standard
590 chow), relative to their respective pre-KD controls. Namely, differentially abundant metabolites
591 related to metabolism of methionine, glycine, serine, and betaine were shared across post-KD
592 conditions for human donor and microbiota-recipient mice. Methionine metabolism involves the
593 production of homocysteine, adenosine, cysteine, and alpha-ketobutyrate, which can then be
594 routed to glucogenic pathways by conversion to propionyl- and succinyl-CoA. Serine, synthesized
595 via glycerate, is used to create glycine (and cysteine) via the homocysteine cycle, which can
596 undergo microbial conversion into pyruvate or glyoxylate. Betaine (trimethylglycine), derived from
597 diet or synthesized from choline, is metabolized by the gut microbiome (Koistinen et al., 2019)
598 and functions as a methyl donor in transmethylation reactions, including those involved in
599 methionine metabolism. While the relevance to KD and seizure protection is unclear, alterations
600 in peripheral and central amino acid metabolism have been widely implicated in mediating the
601 anti-seizure effects of the KD (Yudkoff et al., 2001). In addition, post-KD samples from both human
602 donors and mouse recipients exhibited alterations in chemicals related to lipid metabolism, such
603 as hydroxy fatty acids. The shared metabolite pathway- and chemical subclass-level features may
604 reflect changes that are induced by KD in humans and generally phenocopied by gut microbes
605 upon transfer to mice reared under non-ketogenic conditions. This suggests that transfer of
606 clinical KD-induced gut microbes to mice maintained under non-ketogenic conditions could result
607 in molecular outputs that are distinct, but functionally similar, to those seen in the donor human
608 sample.
609
610 We observed that inoculating mice with human fecal samples collected after clinical KD treatment
611 conferred resistance to 6-Hz seizures compared to controls that received the baseline pre-

612 treatment (pre-KD) microbiota. There was no correlation with patient responsiveness to diet, as
613 indicated in clinician notes taken at 1 month after adherence to the clinical KD. This may be due
614 to the unreliability of the metric, which was based on parental reporting, as well as the cross-
615 sectional nature of the assessment, given inter-individual variation in latency to respond to KD
616 treatments and the patient's peak KD ratio. These concerns aside, the results highlight the
617 importance of host determinants of KD responsiveness, some of which may mask or block any
618 beneficial influences of the KD-associated microbiota. Many patients included in this study
619 exhibited genetic bases for refractory epilepsy, some of which could be epistatic to functional
620 genomic changes in the KD-associated gut microbiome. Large human studies that subclassify
621 different types of epilepsies and seizure semiologies are warranted to study potential roles for the
622 gut microbiome in modifying or predicting responsiveness to the KD.
623
624 The microbiota-dependent increases in seizure protection were associated with brain
625 transcriptomic alterations. In particular, both hippocampus and frontal cortex from post-KD
626 recipient mice exhibited enrichment of differentially expressed genes related to i) RNA processing,
627 transcriptional regulation, and translation ii) TORC1 signaling and cell cycle, and iii) oxidative
628 phosphorylation and cellular stress response (i.e., nitric oxide, reactive oxygen species), when
629 compared to controls colonized with pre-KD microbiota from both GO enrichment and STRING
630 network analyses. Neuronal excitability requires protein synthesis in response to altered neuronal
631 stimulation, and risk factors for various epilepsies include dysregulation of RNA processing, RNA
632 stability, transcription, and translation (Malone & Kaczmarek, 2022). TORC1 is a major nutrient-
633 and energy-sensing serine/threonine kinase complex that controls cell growth and differentiation
634 by coordinating core processes of transcription, translation, and autophagy. Abnormal regulation
635 of TORC1 signaling has been implicated in a wide variety of epilepsies, and as such, is a
636 therapeutic target of interest for treating refractory epilepsies (Nguyen & Bordey, 2021). Previous
637 studies have reported inhibitory effects of the KD and select fatty acids on TORC1 activity

638 (McDaniel et al., 2011; Warren et al., 2020), suggesting that it may contribute to the anti-seizure
639 effects of the KD. Oxidative phosphorylation is a central process for cellular energy metabolism
640 from nutrients, that generates as a byproduct reactive oxygen species (ROS) (Rowley & Patel,
641 2013) and is regulated by the retrograde glutamatergic neurotransmitter nitric oxide (NO). In
642 animal epilepsy models, both ROS and NO are elevated during seizure activity due to oxidative
643 stress-associated neuronal death (Zhu et al., 2017), which can further contribute to
644 epileptogenesis (Chan, 2001). The KD has been previously reported to reduce oxidative stress
645 by promoting antioxidant enzymatic activity and scavenging ROS (Greco et al., 2016). Overall,
646 these results suggest that the KD-associated human gut microbiota alters brain transcriptional
647 pathways that may contribute to protection against 6-Hz seizures in mice.
648
649 Integration of multi'omics datasets across human donor and mouse recipients revealed network
650 associations between select gut microbial metagenomic pathways, fecal metabolites, serum
651 metabolites, and hippocampal transcripts, suggesting that they may contribute to the microbiome-
652 dependent increases in seizure protection seen in mice inoculated with human post-KD
653 microbiota, compared to pre-KD controls. The human donor and mouse recipient co-occurrence
654 networks were linked by shared metagenomic pathway nodes related to BCAA biosynthesis, CoA
655 biosynthesis, L-alanine fermentation, and L-arginine biosynthesis. Key drivers for BCAA, CoA,
656 and L-arginine biosynthesis were linked to hippocampal transcript modules enriched for genes
657 related to neurogenesis and Wnt signaling. BCAAs modulate brain import of precursors required
658 for synthesis of monoamine transmitters (Larsson & Markus, 2017; Salcedo et al., 2021; Song et
659 al., 2017). BCAAs also serve as nitrogen donors for synthesis of glutamate vs. GABA, and as
660 such regulates synaptic balance between excitation and inhibition, a key determinant of seizure
661 susceptibility (McKenna et al., 2019). Wnt signaling regulates calcium pathways that are important
662 for hippocampal neurogenesis and dendrite formation, and is increasingly linked to early
663 epileptogenesis (Hodges and Lugo, 2018). Additionally, mapping GWAS-based risk genes to the

664 co-occurrence network identified five hippocampal nodes as linked to epilepsy. Of particular
665 interest was *Gnaz*, which encodes G protein alpha-Z, a protein that mediates neuronal signal
666 transduction within the hippocampus (Jang et al., 2018) and is proposed to modulate seizure
667 susceptibility (Hultman et al., 2019). BCAA derivatives have been reported to promote
668 phosphorylation of G-proteins, and abnormalities in GPCR mediated neuronal signaling can
669 contribute to increased susceptibility to seizure (Shellhammer et al., 2017; Yu et al., 2019).
670 Altogether, results from this study reveal that the clinical KD regimens used to treat pediatric
671 refractory epilepsy are associated with alterations in the function of the child microbiome, which
672 causally modify brain function and seizure susceptibility upon transfer to mice. Further research
673 is warranted to define the mechanisms by which the human KD-associated microbiome signals
674 across the gut-brain axis to modify seizure risk, and to further assess the potential for identifying
675 microbiome-based interventions that could increase the efficacy of KD treatment, alleviate dietary
676 side effects, and/or ease clinical implementation.
677
678 **LIMITATIONS OF STUDY**
679
680 A key limitation of this study design is the prioritization of experimental reproducibility, which
681 included cohorts of 14-16 mice per patient sample, over patient sample size, which included 10
682 children with refractory epilepsy, each sampled before and at approximately 1 month after
683 adherence to a clinical KD. We reasoned that by internally controlling for baseline microbiota for
684 each patient, we could effectively evaluate microbial alterations in response to the clinical KD
685 within a relatively small patient group. We further posited that this study design would enable us
686 to sample from a heterogenous patient population reflective of the etiopathological variation
687 typically seen in refractory epilepsy. It would also us to be inclusive of the wide range of individuals
688 with pediatric epilepsy who typically seek clinical KD treatment. This level of diversity in a small
689 patient population may have contributed to our finding that there was no shared taxonomic

690 response of the gut microbiome to the clinical KD, despite some shared functional genomic
691 features when considering all post-KD microbiota relative to all pre-KD controls.
692
693 Additional constraints of the study, as discussed in the main text, are the inherent technical and
694 biological shortcomings in “transplanting” microbiota across different mammalian hosts. In this
695 study, we achieved levels of human-to-mouse microbiota “transplant” fidelity analogous to those
696 reported in existing literature even when we maintained mice on a conventional rather than
697 ketogenic diet (Bokoliya et al., 2021; Kennedy et al., 2018; Walter et al., 2020). However, the
698 discrepancies between recipient and donor microbiota draw into question the relevance of
699 findings in gnotobiotic mice to the human condition. To help mitigate this, we focused entirely on
700 features of the gut microbiome that were differential between post-KD and pre-KD conditions and
701 shared between human donors and mouse recipients. However, we acknowledge that artifacts of
702 the microbiota transfer approach, which are not relevant to the clinical condition, may contribute
703 to the microbiome-dependent functional differences observed in the gnotobiotic mouse
704 experiments in this study. Nevertheless, the observed results provide important proof-of-principle
705 that differences in the function of the gut microbiota regulate seizure susceptibility.
706
707 In assessing causal relationships between the KD-associated microbiome and host physiologies
708 linked to seizure susceptibility, we made the major assumption that there exists a singular
709 microbiome-dependent mechanism to increase seizure threshold that was common across all
710 post-KD mouse recipient cohorts relative to all pre-KD cohort controls. Our analysis does not take
711 into account the possibility that there are multiple microbiome-dependent mechanisms that are
712 distinct and that each result in resistance to 6-Hz seizures. Expanded studies that involve
713 subclassification of the human participants and/or mouse recipients would aid in addressing this
714 prospect.
715

716 Moreover, we chose to study the 6-Hz psychomotor seizure model based on its widespread use
717 as a model of refractory epilepsy (Kehne et al., 2017), its utility for screening novel antiepileptic
718 drugs (Barton et al., 2001), and its responsiveness to the KD (Hartman et al., 2008). We also
719 reasoned that its measure of acutely induced seizures would preclude confounding effects of
720 chronic genetic mutation or kindling-based models on modifying the gut microbiome (Löscher,
721 2017). Further research is needed to assess roles for the KD-induced gut microbiome in modifying
722 seizures across additional epilepsy models to determine whether particular seizure semiologies
723 or types of epilepsy are more amenable to modulation by the gut microbiome.
724
725 In light of the aforementioned heterogeneity in patient population, small sample size, variation in
726 clinically-guided KD regimens, discrepancies introduced by the microbiota "transplantation"
727 approach, cross-species and diet comparisons (i.e., human on KD, mouse on standard diet), and
728 assumptions adopted for data analysis, our statistical analyses for shotgun metagenomic,
729 untargeted metabolomic, and bulk transcriptomic data were performed with lenient thresholds for
730 differential abundance ($p<0.05$), with a focus on pathway-level signatures that were dependent
731 upon the clinical KD and conferred by the KD-associated microbiota. Notably, for all animal
732 experiments, technical replicates per donor sample were averaged, and only the biological (i.e.,
733 donor) N was used for statistical analysis. Despite the expected variability, we detected consistent
734 KD-dependent alterations in microbial genes and metabolites in epileptic children undergoing
735 dietary treatment, and further observed KD- and microbiome-dependent alterations in
736 metagenomic pathways and metabolomic pathways that were shared across human donor and
737 microbiome-recipient mice when using these parameters. Brain transcriptomic signatures were
738 seen when comparing all mouse recipient cohorts receiving the post-KD microbiome (all of which
739 exhibited resistance to 6-Hz seizures) relative to those receiving the pre-KD controls. Finally,
740 results for all seizure testing experiments, which revealed shared phenotypic outcomes for post-
741 KD groups compared to pre-KD groups, were well-powered and analyzed according to

742 conventional statistical methods (Festing & Altman, 2002). All caveats considered, the results
743 from this study extend existing pre-clinical research to provide initial evidence that clinical KD
744 treatments shape the function of the gut microbiome of children with refractory epilepsy in ways
745 that have the potential to causally modify seizure susceptibility. Continued research is warranted
746 to elucidate the particular microbial functional activities that act together to modify signaling across
747 the gut-brain axis to promote seizure protection and to further assess the potential to apply
748 microbiome-based interventions to treat refractory epilepsy.
749

750 **ACKNOWLEDGEMENTS**

751 We thank members of the Hsiao laboratory for their critical review of the manuscript, and members
752 of the UCLA Goodman Luskin Microbiome Center Gnotobiotics Core Facility for technical support.
753 This work was supported by funds from a UCLA Whitcome Fellowship to G.R.L. and National
754 Institute of Neurological Disorders and Stroke (NINDS) grant (#R01 NS115537) to E.Y.H. E.Y.H.
755 is a New York Stem Cell Foundation – Robertson Investigator. Individuals involved in this
756 research were supported in part by the New York Stem Cell Foundation and grant number 2018-
757 191860 from the Chan Zuckerberg Initiative DAF, an advised fund of Silicon Valley Community
758 Foundation. Brain RNA sequencing and a subset of metagenomic sequencing was supported by
759 funds from Bloom Science, Inc. (see Declaration of Interests). None of the funding sources
760 influenced or provided input on data analysis or interpretation.
761

762 **AUTHOR CONTRIBUTIONS**

763 G.R.L., S.M.H, C.A.O., M.B., and J.P. performed the experiments and analyzed the data, B.R.,
764 and J.H.M. led the clinical study. G.R.L., C.A.O., J.H.M., X.Y., and E.Y.H. designed the study,
765 G.R.L. and E.Y.H. wrote the manuscript. All authors discussed the results and commented on the
766 manuscript.
767

DECLARATION OF INTERESTS

Findings reported in the manuscript are the subject of provisional patent application US 63/285,267, owned by UCLA. E.Y.H. has financial interests in Bloom Science. All other authors declare that they have no competing interests.

DIVERSITY AND INCLUSION

We worked to ensure sex balance in the selection of human subjects. One or more of the authors of this paper self-identifies as an underrepresented ethnic minority in science. While citing references scientifically relevant for this work, we also actively worked to promote gender balance in our reference list.

FIGURES AND FIGURE LEGENDS

STAR★METHODS

Detailed methods are provided in the online version of the paper and include the following:

- KEY RESOURCES TABLE
- RESOURCE AVAILABILITY
  - Lead Contact
  - Materials availability
  - Data and code availability
- EXPERIMENTAL MODELS AND SUBJECT DETAILS
  - Human Fecal Samples
  - Mice
- METHOD DETAILS
  - 16S rRNA Gene Sequencing

792 - Fecal Shotgun Metagenomics
793 - Human Donor Fecal Microbiota Transfer
794 - 6-Hz Psychomotor Seizure Assay
795 - Antibiotic Treatment
796 - Fecal and Serum Metabolomics
797 - Transcriptomics
798 - Multi'omics Integration
799 - Marker set enrichment analysis (MSEA) to connect hippocampus and frontal cortex DEGs
800 with epilepsy GWAS
801 - QUANTIFICATION AND STATISTICAL ANALYSIS
802

803 ## KEY RESOURCES TABLE

REAGENT or RESOURCE	SOURCE	IDENTIFIER
Biological samples		
Stool samples from human subjects	This study	N/A
Chemicals, Peptides, and Recombinant Proteins		
Vancomycin hydrochloride	Chem-Impex International	00315
Neomycin trisulfate salt hydrate	Sigma-Aldrich	N1876
Metronidazole	Sigma-Aldrich	M1547
Ampicillin sodium salt	Sigma-Aldrich	A9518
TURBO DNase	Invitrogen	AM2238
Ultrapure water	ThermoFisher	10977015
1x PBS	ThermoFisher	10010023
Tetracaine Hydrochloride Opthalmic Solution, USP 0.5%	Oceanside Pharmaceuticals	68682-920-64

Critical Commercial Assays		
DNeasy PowerSoil Kit	Qiagen	12888-50
Qiaquick PCR purification kit	Qiagen	28104
PureLink RNA Mini Kit	Invitrogen	12183018A
QuantSeq FWD' mRNA-Seq Library Prep Kit	Lexogen	N/A
Deposited Data		
16S rRNA gene sequencing	https://qiita.ucsd.edu	14928
Metagenomic sequencing	https://qiita.ucsd.edu	14928
Untargeted metabolomics	https://data.mendeley.com/	DOI:10.17632/djzyzdbz3z.1
Hippocampal transcriptomics	Gene Expression Omnibus	GSE225682
Frontal cortex transcriptomics	Gene Expression Omnibus	GSE225682
WGCNA modules	Github	https://github.com/smha118/keto_diet_pediatric_epilepsy
Experimental Models: Organisms/Strains		
Swiss Webster	Taconic Farms	TAC-SW
Oligonucleotides		
Forward primer for digital PCR: UN00F2, 5′-CAGCMGCCGCGGTAA-3	Integrated DNA Technologies	N/A
Reverse primer for digital PCR: UN00R0, 5′-GGACTACHVGGGTWTCTAAT-3′ [1, 3])	Integrated DNA Technologies	N/A
Software and Algorithms		

Deblur	https://github.com/biocore/deblur	(Amir et al., 2017)
QIIME2-2022.2	https://qiime2.org/	(Bolyen et al., 2019)
FastQC v. 0.11.9	https://github.com/s-andrews/FastQC/releases/tag/v0.11.9	(Andrews, 2010)
ANCOM	https://github.com/FrederickHuangLin/ANCOM-Code-Archive	(Mandal et al., 2015)
Trimmomatic	https://github.com/timflutre/trimmomatic	(Bolger et al., 2014)
HISAT2	http://daehwankimlab.github.io/hisat2/	(Kim et al., 2019)
HTSeq-count	https://github.com/htseq/htseq	(Anders et al., 2015)
DESeq2	https://bioconductor.org/packages/release/bioc/html/DESeq2.html	(Love et al., 2014)
RStudio 2022.07.2	https://www.r-project.org/	(RStudio Team, 2021)
bioBakery	https://github.com/biobakery/biobakery	(McIver et al., 2018)
HUMAnN 3.0	https://github.com/biobakery/humann	(Beghini et al., 2021)
MetaPhlAn 3.0	https://github.com/biobakery/MetaPhlAn	(Beghini et al., 2021)

MaAsLin 2.0	https://github.com/biobakery/biobakery/wiki/maaslin2	(Mallick et al., 2021)
file2meco	https://github.com/ChiLiubio/file2meco	(Liu et al., 2022)
MetaboAnalyst 5.0	https://www.metaboanalyst.ca/home.xhtml	(Pang et al., 2021)
Cytoscape	https://cytoscape.org/	(Shannon et al., 2003)
EnrichR	https://maayanlab.cloud/Enrichr/	(Chen et al., 2013; Kuleshov et al., 2016; Z. Xie et al., 2021)
STRING	https://string-db.org/	(Szklarczyk et al., 2019)
WCGNA	https://horvath.genetics.ucla.edu/html/CoexpressionNetwork/Rpackages/WGCNA/	(Langfelder & Horvath, 2008)
MMVEC	https://github.com/biocore/mmvec	(Morton et al., 2019)
wKDA	http://mergeomics.re	(Ding et al.,

	search.idre.ucla.edu/	2021)
BlueBee	Lexogen	1864011
Prism software	GraphPad	v 8.2.1
Other		
"Breeder" chow	Lab Diets	5K52
Control diet	Harlan Teklad	TD.150300
4200 Tapestation System	Agilent	G2991AA
QX200 Droplet Generator	Bio-Rad Laboratories	1864002
ECT Unit	Ugo Basile	57800

804

805

806 ## RESOURCE AVAILABILITY

807 ### Lead Contact

808 Further information and requests for resources and reagents should be directed to and will be

809 fulfilled by the Lead Contact, Elaine Hsiao (ehsiao@g.ucla.edu)

810

811 ### Materials Availability

812 This study did not generate new unique reagents.

813

814 ### Data and Code Availability

815 Data from 16S rRNA gene sequencing, metagenomic profiling, and associated metadata are

816 presented in Tables S2, S3, S5, and S6 are available online through the QIITA repository

817 (https://qiita.ucsd.edu/) with the study accession #14928. Metabolomic data are presented in

818 Tables S7, S8, S9, and S10 and are available online through Mendeley data with

819 DOI:10.17632/djzyzdbz3z.1. Transcriptomic data are presented in Tables S11 and S12 and

820 available online through Gene Expression Omnibus repository with the identification number

821 #GSE225682.

822

823 ## EXPERIMENTAL MODELS AND SUBJECT DETAILS

824 ### Human Subjects

825 This study was approved by UCLA's Institutional Review Board (IRB protocol #15-000453).
826 Pediatric refractory epilepsy patients were screened and enrolled in collaboration with the
827 Ketogenic Diet Program at UCLA Mattel Children's Hospital. Prospective participants who met
828 study criteria were provided information detailing this study by phone and email 1-2 weeks before
829 their pre-diet initiation visit. Prior to enrollment, informed signed consent was provided by all
830 participants and their guardians to the program clinical coordinator during the pre-diet initiation
831 appointment. Subjects were enrolled across diverse seizure semiology and prior medical
832 histories. Inclusion criteria: enrolled in UCLA's program for classical 4:1 KD, children aged 1-10
833 with refractory epilepsy, any gender, any ethnicity, any previous exposure to AEDs, any seizure
834 semiology. Exclusion criteria: use of antibiotics or probiotics within 7 days prior to enrollment,
835 existing diagnosis of gastrointestinal, immunological, or metabolic disorder. Human donor stool
836 samples were collected from 10 participants, each providing 2 stool samples. The first sample
837 was collected within 1 day before starting KD treatment (pre-KD) and the second sample was
838 collected after maintaining on the clinical KD for 1 month (post-KD). Clinical metadata from the
839 medical record were coded and stripped of identifiers before being shared, and included
840 participant demographic data, medical history, AED exposure history, additional medications take
841 during this study, laboratory blood glucose and bloody ketone body levels, seizure severity,
842 seizure frequency, seizure semiology, and dietary regimen (Table S1).

843

844 ### Human stool sample collection

845 For in-patient fecal sample collection, once a study participant was admitted to the hospital during
846 the pre-diet initiation visit, they were given a coded stool collection kit and sterile specimen

847 container. Stool samples were freshly collected within 1 day prior to starting the clinical KD
848 treatment (pre-KD). Fresh stool samples were immediately placed on dry ice for short term
849 storage and transportation and were freshly frozen at -80°C for long-term storage. Post-KD stool
850 samples were collected in the same manner as stated above when the study participant returned
851 for the 1-month follow-up visit. For out-patient collection of the post-KD stool sample, which was
852 necessitated because of hospital pandemic policies, a deidentified stool sample collection kit and
853 sterile specimen cup was provided to the patient and guardian along with a pre-labeled return
854 shipping box. After 1 month of the clinical KD treatment, stool samples were collected in a sterile
855 specimen cup, immediately placed in an at home freezer, and the next day either (1) shipped
856 back overnight to UCLA on dry ice or (2) brought with the patient to their 1 month follow-up
857 appointment. Fresh frozen fecal samples were homogenized under liquid nitrogen and 3 ~500 mg
858 aliquots were made per sample by sterile storage in anaerobic Balch tubes to be used for
859 transplantation, metagenomic, and metabolomic studies.
860

861 **Mice**

862 6-8 week old wild-type germ-free Swiss Webster mice (Taconic Farms), were bred in UCLA's
863 Center for Health Sciences Barrier Facility. Breeding animals were fed ''breeder'' chow (Lab Diets
864 5K52). Experimental animals were fed vitamin- and mineral-matched control diet (Harlan Teklad
865 TD.150300). Juvenile mice were used to mimic the age range of the human donor population
866 (<10 years old). All animal experiments were approved by the UCLA Animal Care and Use
867 Committee.
868

869 **METHOD DETAILS**

870

871 **16S rRNA Gene Sequencing and Analysis**

872 Bacterial genomic DNA was extracted from human or mouse fecal samples using the Qiagen
873 PowerSoil Kit. For human samples, the n reflects one donor sample. For mouse samples, the n
874 reflects independent cages containing 3 mice per cage to preclude effects of co-housing on
875 microbiota composition. The sequencing library was generated in line with (Caporaso et al.,
876 2011). PCR amplification, run in triplicate, of the V4 region of the 16S rRNA gene was completed
877 using individually barcoded universal primers and 30 ng of the extracted genomic DNA. The PCR
878 product triplicates were pooled and purified using the Qiaquick PCR purification kit (Qiagen).
879 Samples were sequenced using the Illumina MiSeq platform and 2 x 250bp reagent kit for paired-
880 end sequencing at Laragen, Inc. Amplicon sequence variants (ASVs) were chosen by closed
881 reference clustering based on 99% sequence similarity to the SILVA138 database. Taxonomy
882 assignment, rarefaction, and differential abundance testing were performed using QIIME2 2022.2
883 (Bolyen et al., 2019; Mandal et al., 2015).
884
885 **Fecal Shotgun Metagenomics**
886 Bacterial genomic DNA was extracted from human or mouse fecal samples using the Qiagen
887 PowerSoil Kit. 1 ng of DNA was used to prepare DNA libraries using the Nextera XT DNA Library
888 Preparation Kit (Illumina) and genomic DNA was fragmented with Illumina Nextera XT
889 fragmentation enzyme. IDT Unique Dual Indexes were added to each sample before 12 cycles of
890 PCR amplification. AMpure magnetic Beads (Beckman Coulter) were used to purify DNA libraries
891 which were eluted in QIAGEN EB buffer. Qubit 4 fluorometer and Qubit dsDNA HS Assay Kit
892 were used for DNA library quantification. Libraries were then sequenced on Illumina HiSeq 4000
893 platform 2x150bp at a 6M read depth using by CosmosID. Metagenomic data was analyzed using
894 HUMAnN 3.0 (Beghini et al., 2021) and MetaCyc database to profile gene families and pathway
895 abundance. File2meco R package was used for MetaCyc pathway hierarchical classification (Liu
896 et al., 2022). MaAsLin 2.0 (Mallick et al., 2021) was used to assess significant pathway
897 associations between pre-KD and post-KD with a p-value cutoff of 0.1, where $p < 0.05$ pathways

898 are indicated in the figure by asterisk. Heatmaps were generated using the pheatmap v1.0.12
899 package for R.
900
901 **Human Donor Fecal Microbiota Transfer**
902 To prepare collected human stool samples for transplantation studies, the frozen stool sample
903 was pulverized into a powder under liquid nitrogen stream in a sterile heavy-duty foil covered
904 mortar and pestle, aliquoted at 500 mg per tube into 2mL screw cap tubes, and frozen at -80C.
905 A single 500 mg aliquot of human stool sample was entered into a Coy anaerobic chamber and
906 resuspended in pre-reduced 1x PBS + 0.05% L-cysteine. The sample was homogenized using
907 sterile borosilicate glass beads and passed through a 100um filter. GF Swiss Webster mice were
908 colonized by oral gavage of 200 ul fecal suspension. Excess fecal suspension was resuspended
909 and stored at -80C in pre-reduced 1x PBS + 0.05% L-cysteine + 15% glycerol. For administration
910 of fecal filtrates, the fecal suspension was passed through a sterile 0.2 um filter before colonization
911 via oral gavage using 200 ul fecal filtrate.
912
913 **6-Hz Psychomotor Seizure Assay**
914 6-Hz psychomotor seizure assay testing was conducted following Samala et al., 2008. One drop
915 (~50 ul) of 0.5% tetracaine hydrochloride ophthalmic solution was applied to the corneas of each
916 mouse 15 min before stimulation. A thin layer of electrode gel (Parker Signagel) was applied
917 directly to the corneal electrodes and was reapplied before each trial. A constant-current current
918 device (ECT Unit 57800, Ugo Basile) was used to deliver current through the corneal electrodes
919 at 3s duration, 0.2 ms pulse-width and 6 pulses/s frequency. CC50 (the milliamp intensity of
920 current required to elicit seizures in 50% of the mouse cohort) was measured as a metric for
921 seizure susceptibility. Pilot experiments were conducted to identify 28 mA as the CC50 for SPF
922 wild-type Swiss Webster mice, aged 6-8 weeks. Each mouse was seizure-tested only once, and
923 thus at least n > 14 mice were used to adequately power each cohort. To determine CC50s for

924 each tested cohort, 28 mA of current was administered to the first mouse per cohort, followed by
925 stepwise fixed increases or decreases by 2 mA intervals. Mice were restrained manually during
926 stimulation and then released into a new cage for behavioral observation. Quantitative measures
927 for falling, tail dorsiflexion (Straub tail), forelimb clonus, eye/vibrissae twitching and behavioral
928 remission were scored manually. For each behavioral parameter, we observed no correlation
929 between percentage incidence during 28+ mA seizures between pre-KD or post-KD microbiota
930 status, suggesting a primary effect of the microbiota on seizure incidence rather than presentation
931 or form. Latency to exploration (time elapsed from when an experimental mouse is released into
932 the observation cage (after corneal stimulation) to its first lateral movement) was scored manually
933 with an electronic timer. Mice were blindly scored as protected from seizures if they did not show
934 seizure behavior and resumed normal exploratory behavior within 10 s. Seizure threshold (CC50)
935 was determined as previously described (Kimball et al., 1957), using the average log interval of
936 current steps per experimental group, where sample n is defined as the subset of animals
937 displaying the less frequent seizure behavior. Data used to calculate CC50 are also displayed as
938 latency to explore for each current intensity, where n represents the total number of biological
939 replicates per group regardless of seizure outcome.
940

941 **Antibiotic Treatment**

942 Transplanted mice were gavaged with a solution of vancomycin (50 mg/kg), neomycin (100
943 mg/kg) and metronidazole (100 mg/kg) every 12 hours daily for 5 days, as adapted from (Reikvam
944 et al., 2011). Ampicillin (1 mg/ml) was provided *ad libitum* in drinking water. For mock treatment,
945 mice were gavaged with a similar volume of 1x PBS (vehicle) water every 12 hours daily for 7
946 days. Antibiotic-treated mice were maintained in sterile caging with sterile food and water and
947 handled aseptically for the remainder of the experiments.
948

949 **Fecal and Serum Metabolomics**

950 Previously collected human donor fecal samples were aliquoted as described in section “Human
951 Donor Fecal Microbiota Transfer”. Mouse fecal samples were collected from mice housed across
952 independent cages, with four cages housing 3 mice and one cage housing 2 mice. Mouse serum
953 samples were collected by cardiac puncture and separated using SST vacutainer tubes, then
954 frozen at -80C. Samples were prepared using the automated MicroLab STAR system (Hamilton
955 Company) and analyzed on GC/MS, LC/MS and LC/MS/MS platforms by Metabolon, Inc. Protein
956 fractions were removed by serial extractions with organic aqueous solvents, concentrated using
957 a TurboVap system (Zymark) and vacuum dried. For LC/MS and LC-MS/MS, samples were
958 reconstituted in acidic or basic LC-compatible solvents containing > 11 injection standards and
959 run on a Waters ACQUITY UPLC and Thermo-Finnigan LTQ mass spectrometer, with a linear
960 ion-trap frontend and a Fourier transform ion cyclotron resonance mass spectrometer back-end.
961 For GC/MS, samples were derivatized under dried nitrogen using bistrimethyl-silyl-
962 trifluoroacetamide and analyzed on a Thermo-Finnigan Trace DSQ fast-scanning single-
963 quadrupole mass spectrometer using electron impact ionization. Chemical entities were identified
964 by comparison to metabolomic library entries of purified standards. Following log transformation
965 and imputation with minimum observed values for each compound, post-KD vs. pre-KD
966 comparisons for human fecal, and mouse serum and fecal data were analyzed by paired t-test.
967 Metabolomic data from SPF or antibiotic-treated mice fed KD vs. CD chow were acquired from
968 (Olson et al., 2018), as log transformed and imputed with minimum observed values for each
969 compound. Data were analyzed using two-way ANOVA to test for group effects. P and q-values
970 were calculated based on two-way ANOVA contrasts. Principal components analysis was used
971 to visualize variance distributions. Supervised Random Forest analysis was conducted to identify
972 metabolomics prediction accuracies. Metabolite set enrichment analysis (MSEA) using the
973 Metaboanalyst 5.0 platform (Pang et al., 2021) was performed on human fecal, mouse fecal, and
974 mouse serum metabolites statistically significantly altered in post-KD compared to pre-KD (p-

val<0.05). Metabolite sets were analyzed for chemical sub-class enrichment and metabolite pathway enrichment, using The Small Molecule Pathway Database (SMPDB).

Transcriptomics

Recipient mice were sacrificed on day 4 post-colonization. Hippocampal, frontal cortex, were dissected from pre-KD and post-KD recipient mice (n=6 per cohort) and immediately placed in Trizol. RNA was extracted using the PureLink RNA Mini kit with Turbo DNAse treatment. RNA was prepared using the TruSeq RNA Library Prep kit and 2 Å~ 69-bp paired-end sequencing was performed using the Illumina HiSeq 4000 platform by the UCLA Neuroscience Genomics Core. FastQC v0.11.5, bbduk v35.92, and RSeQC v2.6.4 were used for quality filtering, trimming, and mapping. Reads were aligned to UCSC Genome Browser assembly ID: mm10 using STAR v2.5.2a, indexed using samtools v1.3, and aligned using HTSeq-count v0.6.0. Differential expression analysis was conducted using DESeq2 v1.24.041. Heatmaps were generated using the pheatmap v1.0.12 package for R. GO term enrichment analysis of differentially expressed genes with $p < 0.05$ was conducted using enrichR v3.1. Protein interaction networks were generated using STRING v10.5. Functional enrichments of network nodes were categorized by GO: biological process, molecular function, and cellular component.

Multi-omics Integration

To assess the relationships across omics layers, we first carried out dimension reduction for each data set using weighted gene co-expression network analysis (WGCNA v1.72.1) (Langfelder & Horvath, 2008). Metabolomics for human donors and mouse recipients and RNA-seq for mouse recipients (hippocampus and frontal cortex) were used to build WGCNA modules within each dataset, where modules represent clusters of highly co-regulated/expressed molecules which are typically involved in similar biological functions. For metabolomics data, *goodSamplesGenes* function was first used with default parameters to filter out sparse metabolites across samples

1001 before constructing networks; this step was not used for RNAseq data. Standard WGCNA steps
1002 were then carried out for the filtered metabolomics and RNAseq data. Module eigengenes (MEs),
1003 or the first axis of principal component were calculated from each module. MEs were then targeted
1004 for correlation analysis with the metadata (pre-KD vs. post-KD and responder vs. non-responder).
1005 Modules that had significant correlation (p-val <0.05) with the metadata were chosen for
1006 subsequent integrative analysis.
1007
1008 A systematic network that combined all omics data was inferred based on the probability of co-
1009 occurrence (POC) between molecules from different omics data. To calculate POC, we leveraged
1010 a neural-net based tool called MMVEC v1.0.6 with default parameters (Morton et al., 2019). The
1011 subset of raw data that contains module components that were selected from WGCNA analysis
1012 were log normalized and combined based on sample ID. This combined data matrix was then
1013 used as input for MMVEC. For example, on donor side, modules from fecal metagenome and
1014 metabolomics were added together and, on the recipient side, the combined matrix contained the
1015 raw data from metagenome, metabolomics, and RNAseq. Due to high density of the overall
1016 network generated from MMVEC, the top 10% of POC connections were retrieved to minimize
1017 overall complexity of the network for both donors and recipients using in-house python script
1018 (https://github.com/smha118/keto_diet_pediatric_epilepsy).
1019
1020 The networks of modules from individual omics layers from donor (metagenome, metabolomics)
1021 and recipient (metagenome, metabolomics, RNAseq) as well as differentially
1022 expressed/abundance molecules were then seeded into Mergeomics v3.16 pipeline along with
1023 the integrated network generated with MMVEC for weighted key driver analysis (wKDA) to identify
1024 key drivers of the networks (Ding et al., 2021). wKDA uses a $\chi 2$ -like statistic to identify molecules
1025 that are connected to significant larger module components than what would be expected by
1026 random chance. The analysis was done on the human and mouse networks separately. To further

1027 look into the network that are relevant to ketogenic diet and epilepsy, we selected key drivers
1028 (KDs) based on i) the number of modules that a key driver was invoked related to, ii) their relation
1029 to the Ketogenic diet or epilepsy. A subset of nodes in each module that were connected to the
1030 KDs were collected. These nodes were retrieved with following priority i) they are part of
1031 differentially regulated molecules ii) POC value with KDs. Finally, the network was visualized
1032 using Cytoscape (Shannon et al., 2003). To minimize overall density of the network, we chose to
1033 show the key drivers Mergeomics with the highest occurrence in their respective MEs and with >
1034 5 degrees of connectivity.
1035

1036 **Marker set enrichment analysis (MSEA) to connect hippocampus and frontal cortex**
1037 **DEGs with epilepsy GWAS**

1038 To assess the potential role of the DEGs from the hippocampus and frontal cortex in epilepsy, we
1039 collected the summary statistics of the latest epilepsy GWAS (Abou-Khalil et al., 2018). Single
1040 nucleotide polymorphisms (SNPs) that had a linkage disequilibrium of $r^2 > 0.5$ were filtered to
1041 remove redundancies. To map the epilepsy GWAS SNPs to genes, we used GTEx version 8
1042 eQTL and sQTL data for brain hippocampus and brain frontal cortex (Aguet et al., 2020), which
1043 help us derive genes likely to be regulated by the SNPs. We next used the MSEA function of the
1044 Mergeomics package (Ding et al., 2021) to compare epilepsy disease association p-values of the
1045 SNPs representing the DEGs (hippocampus or frontal cortex) with those of the SNPs mapped to
1046 random genes to assess whether the DEGs contain SNPs that show stronger epilepsy association
1047 than random genes using a χ^2-like statistic.
1048

1049 **QUANTIFICATION AND STATISTICAL ANALYSIS**

1050 Statistical analyses were conducted using Prism8 software v8.2.1 (GraphPad). Before statistical
1051 analysis, data was assessed for distribution to determine appropriate statistical tests to use. Data
1052 were plotted in figures as mean ± SEM. For figures: 1B, S2C, S3B, S3B, S4C, *n* = the number of

technical replicates. For all other figures, *n* = the number of biological replicates. No samples or animals were excluded from data analysis. Differences between two sample conditions from parametric data sets were analyzed using two-tailed, paired Student's t-test. Differences between two sample conditions from nonparametric data sets were analyzed using two-tailed, Wilcoxon matched-pairs signed rank test. For differences among >2 groups when analyzing one variable, a one-way ANOVA with Tukey's post hoc test was used. For differences among ≥2 groups with two variables, a two-way ANOVA with Sidak's post hoc test was used. For technical replicates from within-patient analysis (Figures: 1B, S2C, S3B, S3B, S4C), differences from the above tests are denoted by: $^{\#}p<0.05$; $^{\#\#}p<0.01$; $^{\#\#\#}p<0.001$; $^{\#\#\#\#}p<0.0001$. For biological replicates (all other figures), differences from the above tests are denoted by: $^{*}p<0.05$; $^{**}p<0.01$; $^{***}p<0.001$; $^{****}p<0.0001$. Non-significant differences are denoted in the figures using "n.s".

SUPPLEMENTAL INFORMATION

Supplemental Information includes seven figures and fourteen tables that contain source data and can be found with this article.

REFERENCES

Abou-Khalil, B., Auce, P., Avbersek, A., Bahlo, M., Balding, D. J., Bast, T., Baum, L., Becker, A. J., Becker, F., Berghuis, B., Berkovic, S. F., Boysen, K. E., Bradfield, J. P., Brody, L. C., Buono, R. J., Campbell, E., Cascino, G. D., Catarino, C. B., Cavalleri, G. L., … Zimprich, F. (2018). Genome-wide mega-analysis identifies 16 loci and highlights diverse biological mechanisms in the common epilepsies. *Nature Communications*, *9*(1). https://doi.org/10.1038/s41467-018-07524-z

Abrams, G. D., & Bishop, J. E. (1967). Effect of the Normal Microbial Flora on Gastrointestinal Motility. *Proceedings of the Society for Experimental Biology and Medicine*, *126*(1). https://doi.org/10.3181/00379727-126-32430

Aguet, F., Barbeira, A. N., Bonazzola, R., Brown, A., Castel, S. E., Jo, B., Kasela, S., Kim-Hellmuth, S., Liang, Y., Oliva, M., Flynn, E. D., Parsana, P., Fresard, L., Gamazon, E. R., Hamel, A. R., He, Y., Hormozdiari, F., Mohammadi, P., Muñoz-Aguirre, M., … Volpi, S. (2020). The GTEx Consortium atlas of genetic regulatory effects across human tissues. *Science*, *369*(6509). https://doi.org/10.1126/SCIENCE.AAZ1776

Ahn, S., Jung, J., Jang, I. A., Madsen, E. L., & Park, W. (2016). Role of glyoxylate shunt in oxidative stress response. *Journal of Biological Chemistry*, *291*(22). https://doi.org/10.1074/jbc.M115.708149

Amir, A., McDonald, D., Navas-Molina, J. A., Kopylova, E., Morton, J. T., Zech Xu, Z., Kightley, E. P., Thompson, L. R., Hyde, E. R., Gonzalez, A., & Knight, R. (2017). Deblur Rapidly Resolves Single-Nucleotide Community Sequence Patterns. *MSystems*, *2*(2). https://doi.org/10.1128/msystems.00191-16

Anders, S., Pyl, P. T., & Huber, W. (2015). HTSeq-A Python framework to work with high-throughput sequencing data. *Bioinformatics*, *31*(2). https://doi.org/10.1093/bioinformatics/btu638

Andrews, S. (2010). FastQC - A quality control tool for high throughput sequence data. http://www.bioinformatics.babraham.ac.uk/projects/fastqc/. *Babraham Bioinformatics*.

Ang, Q. Y., Alexander, M., Newman, J. C., Tian, Y., Cai, J., Upadhyay, V., Turnbaugh, J. A., Verdin, E., Hall, K. D., Leibel, R. L., Ravussin, E., Rosenbaum, M., Patterson, A. D., & Turnbaugh, P. J. (2020). Ketogenic Diets Alter the Gut Microbiome Resulting in Decreased Intestinal Th17 Cells. *Cell*, *181*(6). https://doi.org/10.1016/j.cell.2020.04.027

Arrington, D. D., van Vleet, T. R., & Schnellmann, R. G. (2006). Calpain 10: A mitochondrial calpain and its role in calcium-induced mitochondrial dysfunction. *American Journal of Physiology - Cell Physiology*, *291*(6). https://doi.org/10.1152/ajpcell.00207.2006

Barton, M. E., Klein, B. D., Wolf, H. H., & White, H. S. (2001). Pharmacological characterization of the 6 Hz psychomotor seizure model of partial epilepsy. *Epilepsy Research*, *47*(3). https://doi.org/10.1016/S0920-1211(01)00302-3

Beghini, F., McIver, L. J., Blanco-Míguez, A., Dubois, L., Asnicar, F., Maharjan, S., Mailyan, A., Manghi, P., Scholz, M., Thomas, A. M., Valles-Colomer, M., Weingart, G., Zhang, Y., Zolfo, M., Huttenhower, C., Franzosa, E. A., & Segata, N. (2021). Integrating taxonomic, functional, and strain-level profiling of diverse microbial communities with biobakery 3. *ELife*, *10*. https://doi.org/10.7554/eLife.65088

Blanton, L. v., Charbonneau, M. R., Salih, T., Barratt, M. J., Venkatesh, S., Ilkaveya, O., Subramanian, S., Manary, M. J., Trehan, I., Jorgensen, J. M., Fan, Y. M., Henrissat, B., Leyn, S. A., Rodionov, D. A., Osterman, A. L., Maleta, K. M., Newgard, C. B., Ashorn, P., Dewey, K. G., & Gordon, J. I. (2016). Gut bacteria that prevent growth impairments transmitted by microbiota from malnourished children. *Science*, *351*(6275). https://doi.org/10.1126/science.aad3311

Blechynden, L. M., Lawson, C. M., & Garlepp, M. J. (1996). Sequence and polymorphism analysis of the murine gene encoding histidyl-tRNA synthetase. *Gene*, *178*(1–2). https://doi.org/10.1016/0378-1119(96)00358-7

Bokoliya, S. C., Dorsett, Y., Panier, H., & Zhou, Y. (2021). Procedures for Fecal Microbiota Transplantation in Murine Microbiome Studies. In *Frontiers in Cellular and Infection Microbiology* (Vol. 11). https://doi.org/10.3389/fcimb.2021.711055

Bolger, A. M., Lohse, M., & Usadel, B. (2014). Trimmomatic: A flexible trimmer for Illumina sequence data. *Bioinformatics*, *30*(15). https://doi.org/10.1093/bioinformatics/btu170

Bolyen, E., Rideout, J. R., Dillon, M. R., Bokulich, N. A., Abnet, C. C., Al-Ghalith, G. A., Alexander, H., Alm, E. J., Arumugam, M., Asnicar, F., Bai, Y., Bisanz, J. E., Bittinger, K., Brejnrod, A., Brislawn, C. J., Brown, C. T., Callahan, B. J., Caraballo-Rodríguez, A. M., Chase, J., … Caporaso, J. G. (2019). Reproducible, interactive, scalable and extensible microbiome data science using QIIME 2. In *Nature Biotechnology*. https://doi.org/10.1038/s41587-019-0209-9

Caporaso, J. G., Lauber, C. L., Walters, W. A., Berg-Lyons, D., Lozupone, C. A., Turnbaugh, P. J., Fierer, N., & Knight, R. (2011). Global patterns of 16S rRNA diversity at a depth of millions of sequences per sample. *Proceedings of the National Academy of Sciences of the United States of America*, *108*(SUPPL. 1). https://doi.org/10.1073/pnas.1000080107

Cekanaviciute, E., Yoo, B. B., Runia, T. F., Debelius, J. W., Singh, S., Nelson, C. A., Kanner, R., Bencosme, Y., Lee, Y. K., Hauser, S. L., Crabtree-Hartman, E., Sand, I. K., Gacias, M., Zhu, Y., Casaccia, P., Cree, B. A. C., Knight, R., Mazmanian, S. K., & Baranzini, S. E. (2017). Gut bacteria from multiple sclerosis patients modulate human T cells and exacerbate symptoms in mouse models. *Proceedings of the National Academy of Sciences of the United States of America*, *114*(40). https://doi.org/10.1073/pnas.1711235114

Chan, P. H. (2001). Reactive oxygen radicals in signaling and damage in the ischemic brain. In *Journal of Cerebral Blood Flow and Metabolism* (Vol. 21, Issue 1). https://doi.org/10.1097/00004647-200101000-00002

Chauhan, P., Philip, S. E., Chauhan, G., & Mehra, S. (2022). The Anatomical Basis of Seizures. In *Epilepsy*. https://doi.org/10.36255/exon-publications-epilepsy-anatomical-basis

1153 Chen, E. Y., Tan, C. M., Kou, Y., Duan, Q., Wang, Z., Meirelles, G. v., Clark, N. R., &
1154 Ma'ayan, A. (2013). Enrichr: Interactive and collaborative HTML5 gene list enrichment
1155 analysis tool. *BMC Bioinformatics*, *14*. https://doi.org/10.1186/1471-2105-14-128
1156 Cheng, H., Pablico, S. J., Lee, J., Chang, J. S., & Yu, S. (2020). Zinc Finger Transcription
1157 Factor Zbtb16 Coordinates the Response to Energy Deficit in the Mouse
1158 Hypothalamus. *Frontiers in Neuroscience*, *14*.
1159 https://doi.org/10.3389/fnins.2020.592947
1160 Clark, D. P., & Cronan, J. E. (2005). Two-Carbon Compounds and Fatty Acids as Carbon
1161 Sources. *EcoSal Plus*, *1*(2). https://doi.org/10.1128/ecosalplus.3.4.4
1162 Coppola, G., Veggiotti, P., Cusmai, R., Bertoli, S., Cardinali, S., Dionisi-Vici, C., Elia, M.,
1163 Lispi, M. L., Sarnelli, C., Tagliabue, A., Toraldo, C., & Pascotto, A. (2002). The
1164 ketogenic diet in children, adolescents and young adults with refractory epilepsy: An
1165 Italian multicentric experience. *Epilepsy Research*, *48*(3).
1166 https://doi.org/10.1016/S0920-1211(01)00315-1
1167 Cordaux, R., Udit, S., Batzer, M. A., & Feschotte, C. (2006). Birth of a chimeric primate
1168 gene by capture of the transposase gene from a mobile element. *Proceedings of the*
1169 *National Academy of Sciences of the United States of America*, *103*(21).
1170 https://doi.org/10.1073/pnas.0601161103
1171 Craddock, K. E., Okur, V., Wilson, A., Gerkes, E. H., Ramsey, K., Heeley, J. M., Juusola,
1172 J., Vitobello, A., Dupeyron, M. N. B., Faivre, L., & Chung, W. K. (2019). Clinical and
1173 genetic characterization of individuals with predicted deleterious PHIP variants. *Cold*
1174 *Spring Harbor Molecular Case Studies*, *5*(4). https://doi.org/10.1101/mcs.a004200
1175 David, L. A., Maurice, C. F., Carmody, R. N., Gootenberg, D. B., Button, J. E., Wolfe, B. E.,
1176 Ling, A. v., Devlin, A. S., Varma, Y., Fischbach, M. A., Biddinger, S. B., Dutton, R. J.,
1177 & Turnbaugh, P. J. (2014). Diet rapidly and reproducibly alters the human gut
1178 microbiome. *Nature*, *505*(7484). https://doi.org/10.1038/nature12820

de Saram, P., Iqbal, A., Murdoch, J. N., & Wilkinson, C. J. (2017). BCAP is a centriolar satellite protein and inhibitor of ciliogenesis. *Journal of Cell Science*, *130*(19). https://doi.org/10.1242/jcs.196642

Dennis, D. J., Han, S., & Schuurmans, C. (2019). bHLH transcription factors in neural development, disease, and reprogramming. In *Brain Research* (Vol. 1705). https://doi.org/10.1016/j.brainres.2018.03.013

Ding, J., Blencowe, M., Nghiem, T., Ha, S. M., Chen, Y. W., Li, G., & Yang, X. (2021). Mergeomics 2.0: A web server for multi-omics data integration to elucidate disease networks and predict therapeutics. *Nucleic Acids Research*, *49*(W1). https://doi.org/10.1093/nar/gkab405

Dolan, S. K., Wijaya, A., Geddis, S. M., Spring, D. R., Silva-Rocha, R., & Welch, M. (2018). Loving the poison: The methylcitrate cycle and bacterial pathogenesis. In *Microbiology (United Kingdom)* (Vol. 164, Issue 3). https://doi.org/10.1099/mic.0.000604

Ducker, G. S., & Rabinowitz, J. D. (2017). One-Carbon Metabolism in Health and Disease. In *Cell Metabolism* (Vol. 25, Issue 1). https://doi.org/10.1016/j.cmet.2016.08.009

Festing, M. F. W., & Altman, D. G. (2002). Guidelines for the design and statistical analysis of experiments using laboratory animals. *ILAR Journal*, *43*(4). https://doi.org/10.1093/ilar.43.4.244

Freeman, J. M., Vining, E. P. G., Pillas, D. J., Pyzik, P. L., Casey, J. C., & Kelly, M. T. (1998). The efficacy of the ketogenic diet - 1998: A prospective evaluation of intervention in 150 children. *Pediatrics*, *102*(6). https://doi.org/10.1542/peds.102.6.1358

Ge, S., Pradhan, D. A., Ming, G. li, & Song, H. (2007). GABA sets the tempo for activity-dependent adult neurogenesis. In *Trends in Neurosciences* (Vol. 30, Issue 1). https://doi.org/10.1016/j.tins.2006.11.001

1204 Götz, M., Nakafuku, M., & Petrik, D. (2016). Neurogenesis in the developing and adult
1205 brain—similarities and key differences. *Cold Spring Harbor Perspectives in Biology*,
1206 *8*(7). https://doi.org/10.1101/cshperspect.a018853
1207 Greco, T., Glenn, T. C., Hovda, D. A., & Prins, M. L. (2016). Ketogenic diet decreases
1208 oxidative stress and improves mitochondrial respiratory complex activity. *Journal of*
1209 *Cerebral Blood Flow and Metabolism*, *36*(9).
1210 https://doi.org/10.1177/0271678X15610584
1211 Green, J. A., & Mykytyn, K. (2014). Neuronal primary cilia: An underappreciated signaling
1212 and sensory organelle in the brain. In *Neuropsychopharmacology* (Vol. 39, Issue 1).
1213 https://doi.org/10.1038/npp.2013.203
1214 Hartman, A. L., Lyle, M., Rogawski, M. A., & Gasior, M. (2008). Efficacy of the ketogenic
1215 diet in the 6-Hz seizure test. *Epilepsia*, *49*(2). https://doi.org/10.1111/j.1528-
1216 1167.2007.01430.x
1217 Hatta, T., Iemura, S. ichiro, Ohishi, T., Nakayama, H., Seimiya, H., Yasuda, T., Iizuka, K.,
1218 Fukuda, M., Takeda, J., Natsume, T., & Horikawa, Y. (2018). Calpain-10 regulates
1219 actin dynamics by proteolysis of microtubule-associated protein 1B. *Scientific Reports*,
1220 *8*(1). https://doi.org/10.1038/s41598-018-35204-x
1221 Hemingway, C., Freeman, J. M., Pillas, D. J., & Pyzik, P. L. (2001). The ketogenic diet: A
1222 3- to 6-year follow-up of 150 children enrolled prospectively. *Pediatrics*, *108*(4).
1223 https://doi.org/10.1542/peds.108.4.898
1224 Hodges, S. L., & Lugo, J. N. (2018). Wnt/β-catenin signaling as a potential target for novel
1225 epilepsy therapies. In *Epilepsy Research* (Vol. 146).
1226 https://doi.org/10.1016/j.eplepsyres.2018.07.002
1227 Hoon, C. K., Yong, J. K., Dong, W. K., & Heung, D. K. (2005). Efficacy and safety of the
1228 ketogenic diet for intractable childhood epilepsy: Korean multicentric experience.
1229 *Epilepsia*, *46*(2). https://doi.org/10.1111/j.0013-9580.2005.48504.x

1230 Hsiung, A., Naya, F. J., Chen, X., & Shiang, R. (2019). A schizophrenia associated CMYA5
1231 allele displays differential binding with desmin. *Journal of Psychiatric Research*, *111*.
1232 https://doi.org/10.1016/j.jpsychires.2019.01.007
1233 Huasong, G., Zongmei, D., Jianfeng, H., Xiaojun, Q., Jun, G., Sun, G., Donglin, W., &
1234 Jianhong, Z. (2015). Serine protease inhibitor (SERPIN) B1 suppresses cell migration
1235 and invasion in glioma cells. *Brain Research*, *1600*.
1236 https://doi.org/10.1016/j.brainres.2014.06.017
1237 Hubbard, T. D., Liu, Q., Murray, I. A., Dong, F., Miller, C., Smith, P. B., Gowda, K., Lin, J.
1238 M., Amin, S., Patterson, A. D., & Perdew, G. H. (2019). Microbiota Metabolism
1239 Promotes Synthesis of the Human Ah Receptor Agonist 2,8-Dihydroxyquinoline.
1240 *Journal of Proteome Research*, *18*(4). https://doi.org/10.1021/acs.jproteome.8b00946
1241 Hultman, R., Boms, O., Mague, S., Hughes, D., Nadler, V., Dzirasa, K., Vasey, P. J.
1242 (2019). A Role for G-alpha-z in regulating seizure susceptibility. *biorxiv*:
1243 https://doi.org/10.1101/567628.
1244 Jang, Y., Moon, J., Lee, S. T., Jun, J. S., Kim, T. J., Lim, J. A., Park, B. S., Yu, J. S., Park,
1245 D. K., Yang, A. R., Park, K. I. I., Jung, K. Y., Kim, M., Jung, K. H., Jeon, D., Chu, K., &
1246 Lee, S. K. (2018). Dysregulated long non-coding RNAs in the temporal lobe epilepsy
1247 mouse model. *Seizure*, *58*. https://doi.org/10.1016/j.seizure.2018.04.010
1248 Jessberger, S., & Parent, J. M. (2015). Epilepsy and adult neurogenesis. *Cold Spring*
1249 *Harbor Perspectives in Biology*, *7*(12). https://doi.org/10.1101/cshperspect.a020677
1250 Joyce, S. A., MacSharry, J., Casey, P. G., Kinsella, M., Murphy, E. F., Shanahan, F., Hill,
1251 C., & Gahan, C. G. M. (2014). Regulation of host weight gain and lipid metabolism by
1252 bacterial bile acid modification in the gut. *Proceedings of the National Academy of*
1253 *Sciences of the United States of America*, *111*(20).
1254 https://doi.org/10.1073/pnas.1323599111

Kehne, J. H., Klein, B. D., Raeissi, S., & Sharma, S. (2017). The National Institute of Neurological Disorders and Stroke (NINDS) Epilepsy Therapy Screening Program (ETSP). *Neurochemical Research*, *42*(7). https://doi.org/10.1007/s11064-017-2275-z

Kennedy, A. R., Pissios, P., Otu, H., Xue, B., Asakura, K., Furukawa, N., Marino, F. E., Liu, F. F., Kahn, B. B., Libermann, T. A., & Maratos-Flier, E. (2007). A high-fat, ketogenic diet induces a unique metabolic state in mice. *American Journal of Physiology - Endocrinology and Metabolism*, *292*(6). https://doi.org/10.1152/ajpendo.00717.2006

Kennedy, E. A., King, K. Y., & Baldridge, M. T. (2018). Mouse microbiota models: Comparing germ-free mice and antibiotics treatment as tools for modifying gut bacteria. *Frontiers in Physiology*, *9*(OCT). https://doi.org/10.3389/fphys.2018.01534

Kim, D., Paggi, J. M., Park, C., Bennett, C., & Salzberg, S. L. (2019). Graph-based genome alignment and genotyping with HISAT2 and HISAT-genotype. *Nature Biotechnology*, *37*(8). https://doi.org/10.1038/s41587-019-0201-4

Kimball, A. W., Burnett, W. T., & Doherty, D. G. (1957). Chemical Protection against Ionizing Radiation: I. Sampling Methods for Screening Compounds in Radiation Protection Studies with Mice. *Radiation Research*. https://doi.org/10.2307/3570549

Koistinen, V. M., Kärkkäinen, O., Borewicz, K., Zarei, I., Jokkala, J., Micard, V., Rosa-Sibakov, N., Auriola, S., Aura, A. M., Smidt, H., & Hanhineva, K. (2019). Contribution of gut microbiota to metabolism of dietary glycine betaine in mice and in vitro colonic fermentation. *Microbiome*, *7*(1). https://doi.org/10.1186/s40168-019-0718-2

Kossoff, E. H., Zupec-Kania, B. A., Auvin, S., Ballaban-Gil, K. R., Christina Bergqvist, A. G., Blackford, R., Buchhalter, J. R., Caraballo, R. H., Cross, J. H., Dahlin, M. G., Donner, E. J., Guzel, O., Jehle, R. S., Klepper, J., Kang, H. C., Lambrechts, D. A., Liu, Y. M. C., Nathan, J. K., Nordli, D. R., … Wirrell, E. C. (2018). Optimal clinical management of children receiving dietary therapies for epilepsy: Updated

recommendations of the International Ketogenic Diet Study Group. *Epilepsia Open*, *3*(2). https://doi.org/10.1002/epi4.12225

Kuleshov, M. v., Jones, M. R., Rouillard, A. D., Fernandez, N. F., Duan, Q., Wang, Z., Koplev, S., Jenkins, S. L., Jagodnik, K. M., Lachmann, A., McDermott, M. G., Monteiro, C. D., Gundersen, G. W., & Maayan, A. (2016). Enrichr: a comprehensive gene set enrichment analysis web server 2016 update. *Nucleic Acids Research*, *44*(1). https://doi.org/10.1093/nar/gkw377

Langfelder, P., & Horvath, S. (2008). WGCNA: An R package for weighted correlation network analysis. *BMC Bioinformatics*, *9*. https://doi.org/10.1186/1471-2105-9-559

Larsson, S. C., & Markus, H. S. (2017). Branched-chain amino acids and Alzheimer's disease: A Mendelian randomization analysis. *Scientific Reports*, *7*(1). https://doi.org/10.1038/s41598-017-12931-1

Leighton, L. J., Zhao, Q., Li, X., Dai, C., Marshall, P. R., Liu, S., Wang, Y., Zajaczkowski, E. L., Khandelwal, N., Kumar, A., Bredy, T. W., & Wei, W. (2018). A Functional Role for the Epigenetic Regulator ING1 in Activity-induced Gene Expression in Primary Cortical Neurons. *Neuroscience*, *369*. https://doi.org/10.1016/j.neuroscience.2017.11.018

Levy, M., Thaiss, C. A., Zeevi, D., Dohnalová, L., Zilberman-Schapira, G., Mahdi, J. A., David, E., Savidor, A., Korem, T., Herzig, Y., Pevsner-Fischer, M., Shapiro, H., Christ, A., Harmelin, A., Halpern, Z., Latz, E., Flavell, R. A., Amit, I., Segal, E., & Elinav, E. (2015). Microbiota-Modulated Metabolites Shape the Intestinal Microenvironment by Regulating NLRP6 Inflammasome Signaling. *Cell*, *163*(6). https://doi.org/10.1016/j.cell.2015.10.048

Lindefeldt, M., Eng, A., Darban, H., Bjerkner, A., Zetterström, C. K., Allander, T., Andersson, B., Borenstein, E., Dahlin, M., & Prast-Nielsen, S. (2019). The ketogenic diet influences taxonomic and functional composition of the gut microbiota in children

with severe epilepsy. *Npj Biofilms and Microbiomes*. https://doi.org/10.1038/s41522-018-0073-2

Liu, C., Li, X., Mansoldo, F. R. P., An, J., Kou, Y., Zhang, X., Wang, J., Zeng, J., Vermelho, A. B., & Yao, M. (2022). Microbial habitat specificity largely affects microbial co-occurrence patterns and functional profiles in wetland soils. *Geoderma*, *418*, 115866. https://doi.org/10.1016/J.GEODERMA.2022.115866

Löscher, W. (2017). Animal Models of Seizures and Epilepsy: Past, Present, and Future Role for the Discovery of Antiseizure Drugs. *Neurochemical Research*, *42*(7). https://doi.org/10.1007/s11064-017-2222-z

Love, M. I., Huber, W., & Anders, S. (2014). Moderated estimation of fold change and dispersion for RNA-seq data with DESeq2. *Genome Biology*, *15*(12). https://doi.org/10.1186/s13059-014-0550-8

Mallick, H., Rahnavard, A., McIver, L. J., Ma, S., Zhang, Y., Nguyen, L. H., Tickle, T. L., Weingart, G., Ren, B., Schwager, E. H., Chatterjee, S., Thompson, K. N., Wilkinson, J. E., Subramanian, A., Lu, Y., Waldron, L., Paulson, J. N., Franzosa, E. A., Bravo, H. C., & Huttenhower, C. (2021). Multivariable association discovery in population-scale meta-omics studies. *PLoS Computational Biology*, *17*(11). https://doi.org/10.1371/journal.pcbi.1009442

Malone, T. J., & Kaczmarek, L. K. (2022). The role of altered translation in intellectual disability and epilepsy. In *Progress in Neurobiology* (Vol. 213). https://doi.org/10.1016/j.pneurobio.2022.102267

Mandal, S., Van Treuren, W., White, R. A., Eggesbø, M., Knight, R., & Peddada, S. D. (2015). Analysis of composition of microbiomes: a novel method for studying microbial composition. *Microbial Ecology in Health & Disease*, *26*(0). https://doi.org/10.3402/mehd.v26.27663

1331 Marchitti, S. A., Orlicky, D. J., & Vasiliou, V. (2007). Expression and initial characterization
1332 of human ALDH3B1. *Biochemical and Biophysical Research Communications*, *356*(3).
1333 https://doi.org/10.1016/j.bbrc.2007.03.046
1334 McDaniel, S. S., Rensing, N. R., Thio, L. L., Yamada, K. A., & Wong, M. (2011). The
1335 ketogenic diet inhibits the mammalian target of rapamycin (mTOR) pathway.
1336 *Epilepsia*, *52*(3). https://doi.org/10.1111/j.1528-1167.2011.02981.x
1337 McIver, L. J., Abu-Ali, G., Franzosa, E. A., Schwager, R., Morgan, X. C., Waldron, L.,
1338 Segata, N., & Huttenhower, C. (2018). BioBakery: A meta'omic analysis environment.
1339 *Bioinformatics*, *34*(7). https://doi.org/10.1093/bioinformatics/btx754
1340 McKenna, M. C., Schuck, P. F., & Ferreira, G. C. (2019). Fundamentals of CNS energy
1341 metabolism and alterations in lysosomal storage diseases. In *Journal of*
1342 *Neurochemistry* (Vol. 148, Issue 5). https://doi.org/10.1111/jnc.14577
1343 Metodiev, M. D., Lesko, N., Park, C. B., Cámara, Y., Shi, Y., Wibom, R., Hultenby, K.,
1344 Gustafsson, C. M., & Larsson, N. G. (2009). Methylation of 12S rRNA Is Necessary for
1345 In Vivo Stability of the Small Subunit of the Mammalian Mitochondrial Ribosome. *Cell*
1346 *Metabolism*, *9*(4). https://doi.org/10.1016/j.cmet.2009.03.001
1347 Mierziak, J., Burgberger, M., & Wojtasik, W. (2021). 3-hydroxybutyrate as a metabolite and
1348 a signal molecule regulating processes of living organisms. In *Biomolecules* (Vol. 11,
1349 Issue 3). https://doi.org/10.3390/biom11030402
1350 Miljanovic, N., & Potschka, H. (2021). The impact of Scn1a deficiency and ketogenic diet
1351 on the intestinal microbiome: A study in a genetic Dravet mouse model. *Epilepsy*
1352 *Research*, *178*. https://doi.org/10.1016/j.eplepsyres.2021.106826
1353 Morton, J. T., Aksenov, A. A., Nothias, L. F., Foulds, J. R., Quinn, R. A., Badri, M. H.,
1354 Swenson, T. L., van Goethem, M. W., Northen, T. R., Vazquez-Baeza, Y., Wang, M.,
1355 Bokulich, N. A., Watters, A., Song, S. J., Bonneau, R., Dorrestein, P. C., & Knight, R.

(2019). Learning representations of microbe–metabolite interactions. *Nature Methods*, *16*(12). https://doi.org/10.1038/s41592-019-0616-3

Mu, C., Choudhary, A., Mayengbam, S., Barrett, K. T., Rho, J. M., Shearer, J., & Scantlebury, M. H. (2022). Seizure modulation by the gut microbiota and tryptophan-kynurenine metabolism in an animal model of infantile spasms. *EBioMedicine*, *76*. https://doi.org/10.1016/j.ebiom.2022.103833

Muda, M., Manning, E. R., Orth, K., & Dixon, J. E. (1999). Identification of the human YVH1 protein-tyrosine phosphatase orthologue reveals a novel zinc binding domain essential for in vivo function. *Journal of Biological Chemistry*, *274*(34). https://doi.org/10.1074/jbc.274.34.23991

Neal, E. G., Chaffe, H., Schwartz, R. H., Lawson, M. S., Edwards, N., Fitzsimmons, G., Whitney, A., & Cross, J. H. (2008). The ketogenic diet for the treatment of childhood epilepsy: a randomised controlled trial. *The Lancet Neurology*, *7*(6). https://doi.org/10.1016/S1474-4422(08)70092-9

Nelson, P. T., Jicha, G. A., Wang, W. X., Ighodaro, E., Artiushin, S., Nichols, C. G., & Fardo, D. W. (2015). ABCC9/SUR2 in the brain: Implications for hippocampal sclerosis of aging and a potential therapeutic target. In *Ageing Research Reviews* (Vol. 24). https://doi.org/10.1016/j.arr.2015.07.007

Nguyen, L. H., & Bordey, A. (2021). Convergent and Divergent Mechanisms of Epileptogenesis in mTORopathies. In *Frontiers in Neuroanatomy* (Vol. 15). https://doi.org/10.3389/fnana.2021.664695

Olson, C. A., Vuong, H. E., Yano, J. M., Liang, Q. Y., Nusbaum, D. J., & Hsiao, E. Y. (2018). The Gut Microbiota Mediates the Anti-Seizure Effects of the Ketogenic Diet. *Cell*. https://doi.org/10.1016/j.cell.2018.04.027

Ott, S. J., Waetzig, G. H., Rehman, A., Moltzau-Anderson, J., Bharti, R., Grasis, J. A., Cassidy, L., Tholey, A., Fickenscher, H., Seegert, D., Rosenstiel, P., & Schreiber, S.

(2017). Efficacy of Sterile Fecal Filtrate Transfer for Treating Patients With Clostridium difficile Infection. *Gastroenterology*, *152*(4). https://doi.org/10.1053/j.gastro.2016.11.010

Özcan, E., Lum, G. R., & Hsiao, E. Y. (2022). Interactions between the gut microbiome and ketogenic diet in refractory epilepsy. *International Review of Neurobiology*, *167*, 217–249. https://doi.org/10.1016/bs.irn.2022.06.002

Pang, Z., Chong, J., Zhou, G., de Lima Morais, D. A., Chang, L., Barrette, M., Gauthier, C., Jacques, P. É., Li, S., & Xia, J. (2021). MetaboAnalyst 5.0: Narrowing the gap between raw spectra and functional insights. *Nucleic Acids Research*, *49*(W1). https://doi.org/10.1093/nar/gkab382

Pánico, P., Salazar, A. M., Burns, A. L., & Ostrosky-Wegman, P. (2014). Role of calpain-10 in the development of diabetes mellitus and its complications. In *Archives of Medical Research* (Vol. 45, Issue 2). https://doi.org/10.1016/j.arcmed.2014.01.005

Puckett, S., Trujillo, C., Wang, Z., Eoh, H., Ioerger, T. R., Krieger, I., Sacchettini, J., Schnappinger, D., Rhee, K. Y., & Ehrt, S. (2017). Glyoxylate detoxification is an essential function of malate synthase required for carbon assimilation in Mycobacterium tuberculosis. *Proceedings of the National Academy of Sciences of the United States of America*, *114*(11). https://doi.org/10.1073/pnas.1617655114

Rawls, J. F., Mahowald, M. A., Ley, R. E., & Gordon, J. I. (2006). Reciprocal Gut Microbiota Transplants from Zebrafish and Mice to Germ-free Recipients Reveal Host Habitat Selection. *Cell*, *127*(2). https://doi.org/10.1016/j.cell.2006.08.043

Reikvam, D. H., Erofeev, A., Sandvik, A., Grcic, V., Jahnsen, F. L., Gaustad, P., McCoy, K. D., Macpherson, A. J., Meza-Zepeda, L. A., & Johansen, F. E. (2011). Depletion of murine intestinal microbiota: Effects on gut mucosa and epithelial gene expression. *PLoS ONE*, *6*(3). https://doi.org/10.1371/journal.pone.0017996

1407 Reinhardt, S., Schuck, F., Stoye, N., Hartmann, T., Grimm, M. O. W., Pflugfelder, G., &
1408 Endres, K. (2019). Transcriptional repression of the ectodomain sheddase ADAM10
1409 by TBX2 and potential implication for Alzheimer's disease. *Cellular and Molecular Life*
1410 *Sciences*, *76*(5). https://doi.org/10.1007/s00018-018-2998-2
1411 Ross, D., & Siegel, D. (2021). The diverse functionality of NQO1 and its roles in redox
1412 control. In *Redox Biology* (Vol. 41). https://doi.org/10.1016/j.redox.2021.101950
1413 Rowley, S., & Patel, M. (2013). Mitochondrial involvement and oxidative stress in temporal
1414 lobe epilepsy. In *Free Radical Biology and Medicine* (Vol. 62).
1415 https://doi.org/10.1016/j.freeradbiomed.2013.02.002
1416 RStudio Team. (2021). RStudio: Integrated Development for R. In *RStudio, Inc., Boston,*
1417 *MA*.
1418 Salcedo, C., Andersen, J. V., Vinten, K. T., Pinborg, L. H., Waagepetersen, H. S., Freude,
1419 K. K., & Aldana, B. I. (2021). Functional Metabolic Mapping Reveals Highly Active
1420 Branched-Chain Amino Acid Metabolism in Human Astrocytes, Which Is Impaired in
1421 iPSC-Derived Astrocytes in Alzheimer's Disease. *Frontiers in Aging Neuroscience*, *13*.
1422 https://doi.org/10.3389/fnagi.2021.736580
1423 Samala, R., Willis, S., & Borges, K. (2008). Anticonvulsant profile of a balanced ketogenic
1424 diet in acute mouse seizure models. *Epilepsy Research*.
1425 https://doi.org/10.1016/j.eplepsyres.2008.05.001
1426 Shannon, P., Markiel, A., Ozier, O., Baliga, N. S., Wang, J. T., Ramage, D., Amin, N.,
1427 Schwikowski, B., & Ideker, T. (2003). Cytoscape: A software Environment for
1428 integrated models of biomolecular interaction networks. *Genome Research*, *13*(11).
1429 https://doi.org/10.1101/gr.1239303
1430 Sharon, G., Cruz, N. J., Kang, D. W., Gandal, M. J., Wang, B., Kim, Y. M., Zink, E. M.,
1431 Casey, C. P., Taylor, B. C., Lane, C. J., Bramer, L. M., Isern, N. G., Hoyt, D. W.,
1432 Noecker, C., Sweredoski, M. J., Moradian, A., Borenstein, E., Jansson, J. K., Knight,

R., … Mazmanian, S. K. (2019). Human Gut Microbiota from Autism Spectrum Disorder Promote Behavioral Symptoms in Mice. *Cell*, *177*(6). https://doi.org/10.1016/j.cell.2019.05.004

Shellhammer, J. P., Morin-Kensicki, E., Matson, J. P., Yin, G., Isom, D. G., Campbell, S. L., Mohney, R. P., & Dohlman, H. G. (2017). Amino acid metabolites that regulate G protein signaling during osmotic stress. *PLoS Genetics*, *13*(5). https://doi.org/10.1371/journal.pgen.1006829

Singh, R. K., Chang, H. W., Yan, D., Lee, K. M., Ucmak, D., Wong, K., Abrouk, M., Farahnik, B., Nakamura, M., Zhu, T. H., Bhutani, T., & Liao, W. (2017). Influence of diet on the gut microbiome and implications for human health. In *Journal of Translational Medicine* (Vol. 15, Issue 1). https://doi.org/10.1186/s12967-017-1175-y

Song, N. N., Huang, Y., Yu, X., Lang, B., Ding, Y. Q., & Zhang, L. (2017). Divergent roles of central serotonin in adult hippocampal neurogenesis. In *Frontiers in Cellular Neuroscience* (Vol. 11). https://doi.org/10.3389/fncel.2017.00185

Sonnenburg, J. L., & Bäckhed, F. (2016). Diet-microbiota interactions as moderators of human metabolism. In *Nature* (Vol. 535, Issue 7610). https://doi.org/10.1038/nature18846

Staley, C., Kaiser, T., Beura, L. K., Hamilton, M. J., Weingarden, A. R., Bobr, A., Kang, J., Masopust, D., Sadowsky, M. J., & Khoruts, A. (2017). Stable engraftment of human microbiota into mice with a single oral gavage following antibiotic conditioning. *Microbiome*, *5*(1). https://doi.org/10.1186/s40168-017-0306-2

Stecker, D., Hoffmann, T., Link, H., Commichau, F. M., & Bremer, E. (2022). L-Proline Synthesis Mutants of Bacillus subtilis Overcome Osmotic Sensitivity by Genetically Adapting L-Arginine Metabolism. *Frontiers in Microbiology*, *13*, 908304. https://doi.org/10.3389/fmicb.2022.908304

Suarez, A. N., Hsu, T. M., Liu, C. M., Noble, E. E., Cortella, A. M., Nakamoto, E. M., Hahn, J. D., de Lartigue, G., & Kanoski, S. E. (2018). Gut vagal sensory signaling regulates hippocampus function through multi-order pathways. *Nature Communications*, *9*(1). https://doi.org/10.1038/s41467-018-04639-1

Szklarczyk, D., Gable, A. L., Lyon, D., Junge, A., Wyder, S., Huerta-Cepas, J., Simonovic, M., Doncheva, N. T., Morris, J. H., Bork, P., Jensen, L. J., & von Mering, C. (2019). STRING v11: Protein-protein association networks with increased coverage, supporting functional discovery in genome-wide experimental datasets. *Nucleic Acids Research*, *47*(D1). https://doi.org/10.1093/nar/gky1131

Tian, L., Wang, X. W., Wu, A. K., Fan, Y., Friedman, J., Dahlin, A., Waldor, M. K., Weinstock, G. M., Weiss, S. T., & Liu, Y. Y. (2020). Deciphering functional redundancy in the human microbiome. *Nature Communications*, *11*(1). https://doi.org/10.1038/s41467-020-19940-1

Turnbaugh, P. J., Ridaura, V. K., Faith, J. J., Rey, F. E., Knight, R., & Gordon, J. I. (2009). The effect of diet on the human gut microbiome: A metagenomic analysis in humanized gnotobiotic mice. *Science Translational Medicine*. https://doi.org/10.1126/scitranslmed.3000322

Venugopal, A. K., Sameer Kumar, G. S., Mahadevan, A., Selvan, L. D. N., Marimuthu, A., Dikshit, J. B., Tata, P., Ramachandra, Y. L., Chaerkady, R., Sinha, S., Chandramouli, B. A., Arivazhagan, A., Satishchandra, P., Shankar, S. K., & Pandey, A. (2012). Transcriptomic profiling of medial temporal lobe epilepsy. *Journal of Proteomics and Bioinformatics*, *5*(2). https://doi.org/10.4172/jpb.1000210

Walter, J., Armet, A. M., Finlay, B. B., & Shanahan, F. (2020). Establishing or Exaggerating Causality for the Gut Microbiome: Lessons from Human Microbiota-Associated Rodents. In *Cell* (Vol. 180, Issue 2). https://doi.org/10.1016/j.cell.2019.12.025

Warren, E. C., Dooves, S., Lugarà, E., Damstra-Oddy, J., Schaf, J., Heine, V. M., Walker, M. C., & Williams, R. S. B. (2020). Decanoic acid inhibits mTORC1 activity independent of glucose and insulin signaling. *Proceedings of the National Academy of Sciences of the United States of America*, *117*(38). https://doi.org/10.1073/pnas.2008980117

Westman, E. C., Feinman, R. D., Mavropoulos, J. C., Vernon, M. C., Volek, J. S., Wortman, J. A., Yancy, W. S., & Phinney, S. D. (2007). Low-carbohydrate nutrition and metabolism. In *American Journal of Clinical Nutrition* (Vol. 86, Issue 2). https://doi.org/10.1093/ajcn/86.2.276

Williams, H. C., Piron, M. A., Nation, G. K., Walsh, A. E., Young, L. E. A., Sun, R. C., & Johnson, L. A. (2020). Oral gavage delivery of stable isotope tracer for in vivo metabolomics. *Metabolites*, *10*(12). https://doi.org/10.3390/metabo10120501

Wu, T., Yin, F., Guang, S., He, F., Yang, L., & Peng, J. (2020). The Glycosylphosphatidylinositol biosynthesis pathway in human diseases. In *Orphanet Journal of Rare Diseases* (Vol. 15, Issue 1). https://doi.org/10.1186/s13023-020-01401-z

Xie, G., Zhou, Q., Qiu, C. Z., Dai, W. K., Wang, H. P., Li, Y. H., Liao, J. X., Lu, X. G., Lin, S. F., Ye, J. H., Ma, Z. Y., & Wang, W. J. (2017). Ketogenic diet poses a significant effect on imbalanced gut microbiota in infants with refractory epilepsy. *World Journal of Gastroenterology*. https://doi.org/10.3748/wjg.v23.i33.6164

Xie, Z., Bailey, A., Kuleshov, M. v., Clarke, D. J. B., Evangelista, J. E., Jenkins, S. L., Lachmann, A., Wojciechowicz, M. L., Kropiwnicki, E., Jagodnik, K. M., Jeon, M., & Ma'ayan, A. (2021). Gene Set Knowledge Discovery with Enrichr. *Current Protocols*, *1*(3). https://doi.org/10.1002/cpz1.90

Yao, J., & Rock, C. O. (2017). Exogenous fatty acid metabolism in bacteria. In *Biochimie* (Vol. 141). https://doi.org/10.1016/j.biochi.2017.06.015

1509 Yassour, M., Vatanen, T., Siljander, H., Hämäläinen, A. M., Härkönen, T., Ryhänen, S. J.,
1510 Franzosa, E. A., Vlamakis, H., Huttenhower, C., Gevers, D., Lander, E. S., Knip, M., &
1511 Xavier, R. J. (2016). Natural history of the infant gut microbiome and impact of
1512 antibiotic treatment on bacterial strain diversity and stability. *Science Translational*
1513 *Medicine*, *8*(343). https://doi.org/10.1126/scitranslmed.aad0917
1514 Yu, Y., Nguyen, D. T., & Jiang, J. (2019). G protein-coupled receptors in acquired epilepsy:
1515 Druggability and translatability. In *Progress in Neurobiology* (Vol. 183).
1516 https://doi.org/10.1016/j.pneurobio.2019.101682
1517 Yudkoff, M., Daikhin, Y., Melø, T. M., Nissim, I., Sonnewald, U., & Nissim, I. (2007). The
1518 ketogenic diet and brain metabolism of amino acids: Relationship to the
1519 anticonvulsant effect. In *Annual Review of Nutrition* (Vol. 27).
1520 https://doi.org/10.1146/annurev.nutr.27.061406.093722
1521 Yudkoff, M., Daikhin, Y., Nissim, I., Lazarow, A., & Nissim, I. (2001). Ketogenic diet, amino
1522 acid metabolism, and seizure control. *Journal of Neuroscience Research*, *66*(5).
1523 https://doi.org/10.1002/jnr.10083
1524 Żarnowska, I., Wróbel-Dudzińska, D., Tulidowicz-Bielak, M., Kocki, T., Mitosek-Szewczyk,
1525 K., Gasior, M., & Turski, W. A. (2019). Changes in tryptophan and kynurenine
1526 pathway metabolites in the blood of children treated with ketogenic diet for refractory
1527 epilepsy. *Seizure*, *69*. https://doi.org/10.1016/j.seizure.2019.05.006
1528 Zhang, T., Dong, K., Liang, W., Xu, D., Xia, H., Geng, J., Najafov, A., Liu, M., Li, Y., Han,
1529 X., Xiao, J., Jin, Z., Peng, T., Gao, Y., Cai, Y., Qi, C., Zhang, Q., Sun, A., Lipinski, M.,
1530 … Yuan, J. (2015). G-protein Coupled Receptors Regulate Autophagy by ZBTB16-
1531 mediated Ubiquitination and Proteasomal Degradation of Adaptor Protein Atg14L.
1532 *ELife*, *2015*(4). https://doi.org/10.7554/eLife.06734

Zhang, Y., Zhou, S., Zhou, Y., Yu, L., Zhang, L., & Wang, Y. (2018). Altered gut microbiome composition in children with refractory epilepsy after ketogenic diet. *Epilepsy Research*. https://doi.org/10.1016/j.eplepsyres.2018.06.015

Zheng, P., Wu, J., Zhang, H., Perry, S. W., Yin, B., Tan, X., Chai, T., Liang, W., Huang, Y., Li, Y., Duan, J., Wong, M. L., Licinio, J., & Xie, P. (2021). The gut microbiome modulates gut–brain axis glycerophospholipid metabolism in a region-specific manner in a nonhuman primate model of depression. *Molecular Psychiatry*, *26*(6). https://doi.org/10.1038/s41380-020-0744-2

Zhou, Y., Holmseth, S., Hua, R., Lehre, A. C., Olofsson, A. M., Poblete-Naredo, I., Kempson, S. A., & Danbolt, N. C. (2012). The betaine-GABA transporter (BGT1, slc6a12) is predominantly expressed in the liver and at lower levels in the kidneys and at the brain surface. *American Journal of Physiology - Renal Physiology*, *302*(3). https://doi.org/10.1152/ajprenal.00464.2011

Zhu, X., Dong, J., Han, B., Huang, R., Zhang, A., Xia, Z., Chang, H., Chao, J., & Yao, H. (2017). Neuronal nitric oxide synthase contributes to PTZ kindling epilepsy-induced hippocampal endoplasmic reticulum stress and oxidative damage. *Frontiers in Cellular Neuroscience*, *11*. https://doi.org/10.3389/fncel.2017.00377

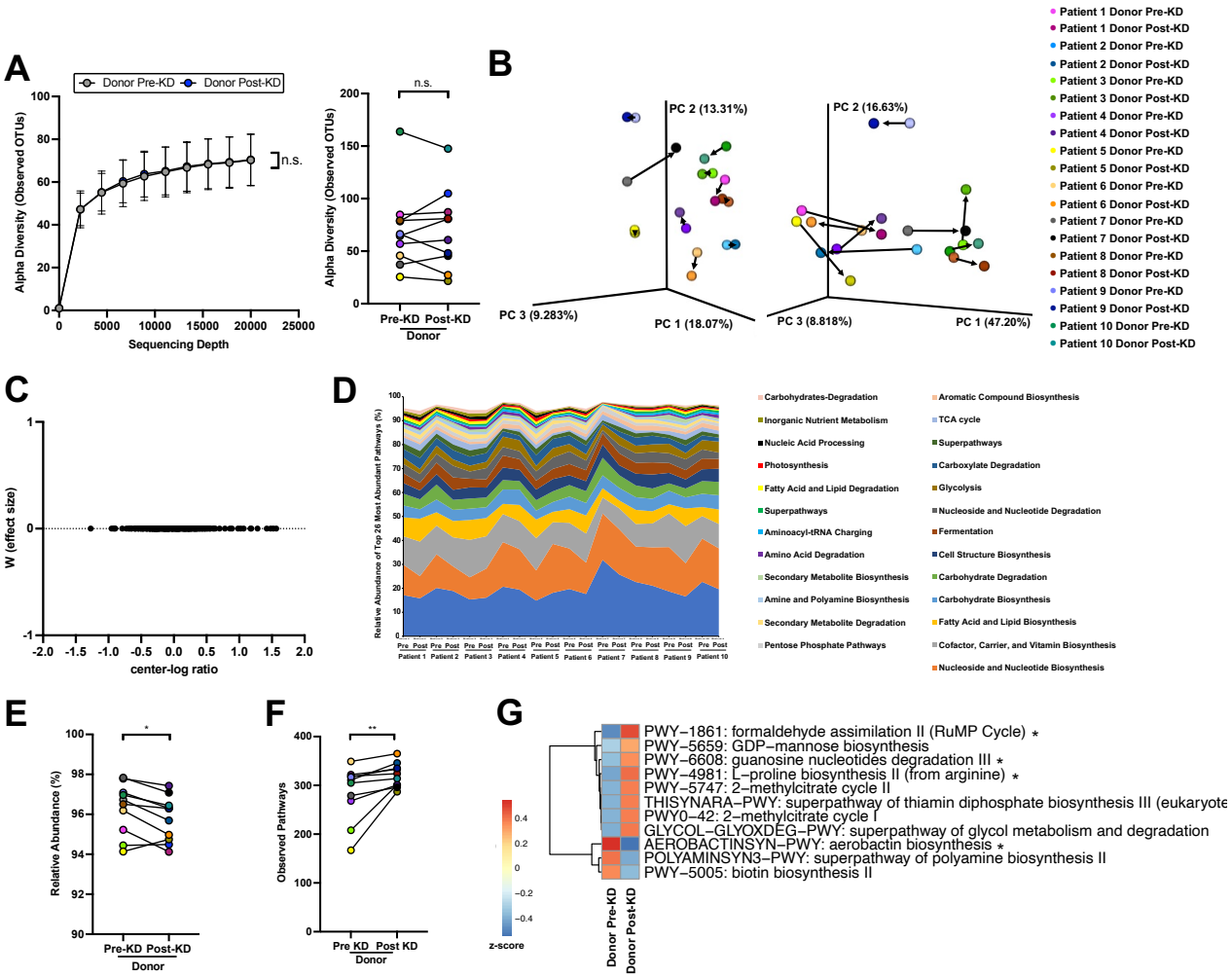

Figure S1: Clinical KD is associated with alterations in the functional potential, but not composition, of the gut microbiota in a cohort of children with refractory epilepsy, Related to Figure 1. **(A)** Alpha diversity as measured by rarefaction curve (left) and observed OTUs (right) of matched donor pre-KD (n=10) and post-KD (n=10) fecal microbiota samples showing no difference in alpha-diversity. (two-way ANOVA with Sidak (left); two-tailed, Wilcoxon matched-pairs signed rank test (right)). **(B)** Principal coordinate analysis of unweighted (left) and weighted (right) UniFrac distances from 16S rRNA gene sequencing of donor pre-KD (n=10) and post-KD (n=10) fecal microbiota samples shifting composition when introduced to the clinical KD. **(C)** ANCOM taxonomic differential abundance testing displaying no differentially abundant taxa by the W score (effect size) metric when comparing donor pre-KD (n=10) and post-KD (n=10). **(D)** Total composition per human donor sample of the top 26 MetaCyc superclass metagenome functional pathways accounting for >94% of relative abundance, for each donor pre-KD (n=10) and post-KD (n=10) fecal microbiota samples. **(E)** Difference in total abundance of the 26 most abundant pathways between matched donor pre-KD (n=10) and post-KD(n=10) fecal microbiota samples (two-tailed, Wilcoxon matched-pairs signed rank test). **(F)** Total number of observed MetaCyc functional pathways in matched donor pre-KD (n=10) and post-KD (n=10) fecal microbiota samples (two-tailed, Wilcoxon matched-pairs signed rank test). **(G)** Heatmap displaying differentially abundant MetaCyc functional pathways associated with donor post-KD (n=10) relative to pre-KD (n=10) by MaAsLin2 analysis with a p-value < 0.1. (pathways with a p-value <0.05 are denoted with *). Data is displayed as mean ± SEM, unless otherwise noted. *p < 0.05, **p < 0.01; KD, ketogenic diet; n.s, no statistical significance.

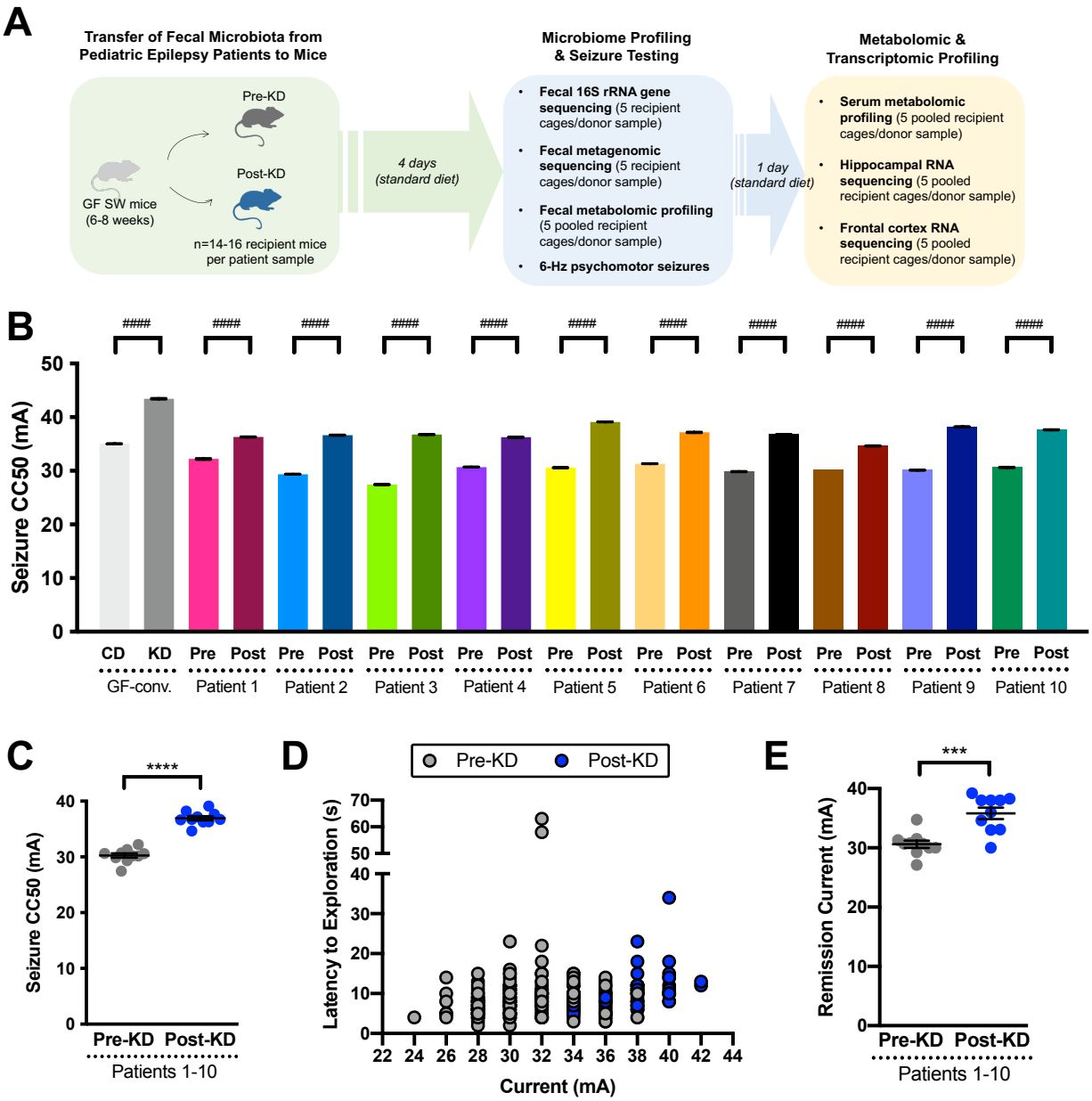

Figure 1: Transfer of the clinical KD-associated gut microbiota from pediatric epilepsy patients to mice confers resistance to 6-Hz seizures. **(A)** Experimental schematic for transplantation of human donor fecal microbiota samples into germ-free (GF) Swiss Webster mice for 6-Hz psychomotor seizure testing. **(B)** 6-Hz seizure thresholds for replicate mice transplanted with human microbiota from paired donor pre-KD and post-KD samples (One-way ANOVA with Tukey's, n = 13-16 mice per patient sample, with # denoting statistical differences when considering within-patient recipient mice as technical replicates). **(C)** Average seizure thresholds of recipient mouse cohorts per patient donor sample. (Two-tailed, unpaired Welch's t-test. n=10 patient samples per group). **(D)** Latency to exploration for all individual pre-KD (n=140) and post-KD (n=141) recipient mice. **(E)** Average current (mA) at which remission seizures were observed per patient donor sample (Two-tailed, unpaired Welch's t-test. n = 10 patient samples per group). Data is displayed as mean ± SEM, unless otherwise noted. #### $p < 0.0001$ (within-patient mouse recipients), ***$p < 0.001$, ****$p < 0.0001$

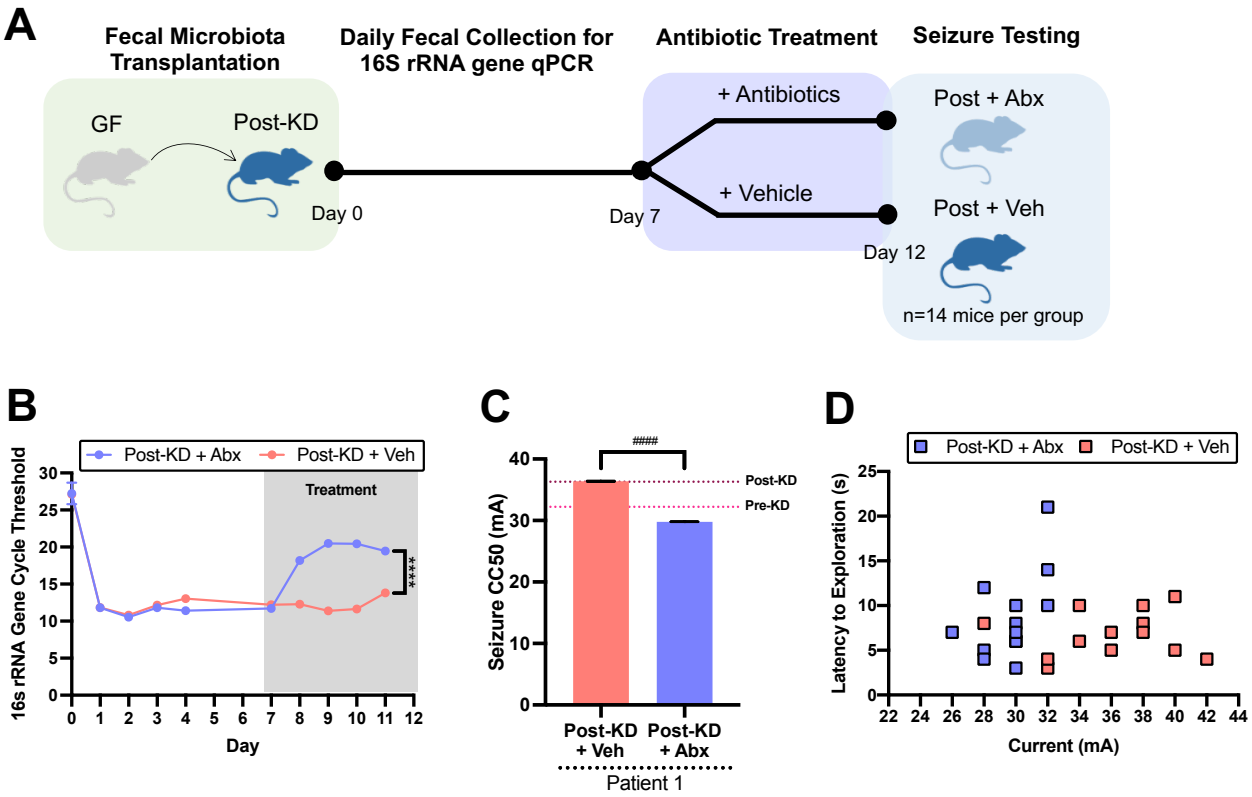

Figure S2: Antibiotic treatment abrogates the seizure protective effects of inoculation with the clinical KD-associated human gut microbiome, Related to Figure 1. (A) Experimental schematic for transfer of human donor fecal microbiota samples to germ-free (GF) mice, followed by 5 days of oral antibiotic (Abx) or vehicle (Veh) treatment, and then 6-Hz psychomotor seizure testing. **(B)** Bacterial loads as measured by quantitative PCR of the 16S rRNA gene from fecal pellets collected once daily before and during Abx or Veh treatment (two-way ANOVA with Sidak, n=3 cages of 3 mice each). **(C)** 6-Hz seizure thresholds for mice inoculated with patient 1 post-KD human microbiota treated with Abx (n=12) or Veh (n=14). Reference lines denote seizure thresholds for mice inoculated with patient 1 post-KD and pre-KD relative control fecal microbiota from Figure 1B (One-way ANOVA with Tukey's, with # denoting statistical differences when considering within-patient recipient mice as technical replicates). **(D)** Latency to exploration for each Abx (n=12) and Veh (n=14) mouse that underwent 6-Hz psychomotor seizure testing. Data is displayed as mean ± SEM, unless otherwise noted. ****$p < 0.0001$. ####$p < 0.0001$ (for within-patient mouse recipients).

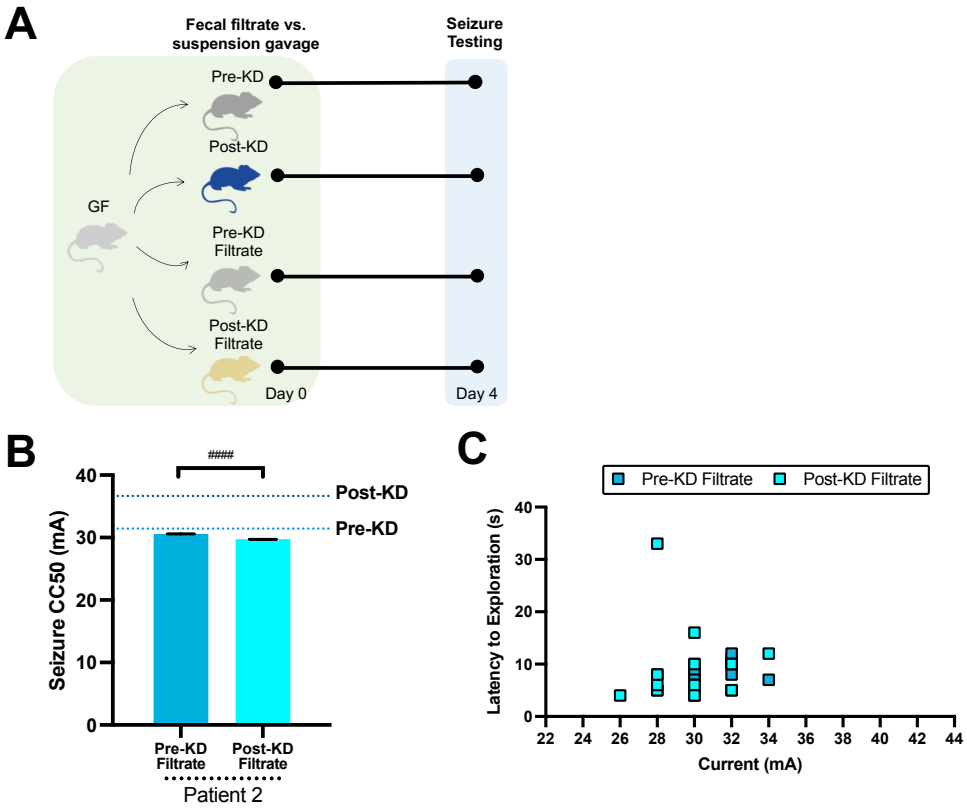

Figure S3: Sterile filtration prevents the seizure protective effects of transfer of the clinical KD-associated human gut microbiome, Related to Figure 1. **(A)** Experimental design for administration of human donor fecal filtrate samples to germ-free (GF) mice, followed by 6-Hz seizure testing 4 days later. **(B)** Seizure thresholds for mice treated with sterile filtered pre-KD (n=14) and sterile filtered post-KD (n=13) fecal samples. Reference lines denote seizure thresholds for mice transplanted with unfiltered patient 2 post-KD and pre-KD relative control fecal microbiota from Figure 1B (One-way ANOVA with Tukey's, with # denoting statistical differences when considering within-patient recipient mice as technical replicates). **(C)** Latency to exploration for mice treated with sterile filtered pre-KD (n=14) and sterile filtered post-KD (n=13) that underwent 6-Hz psychomotor seizure testing. Data is displayed as mean ± SEM, unless otherwise noted. #### $p < 0.0001$ (for within-patient mouse recipients).

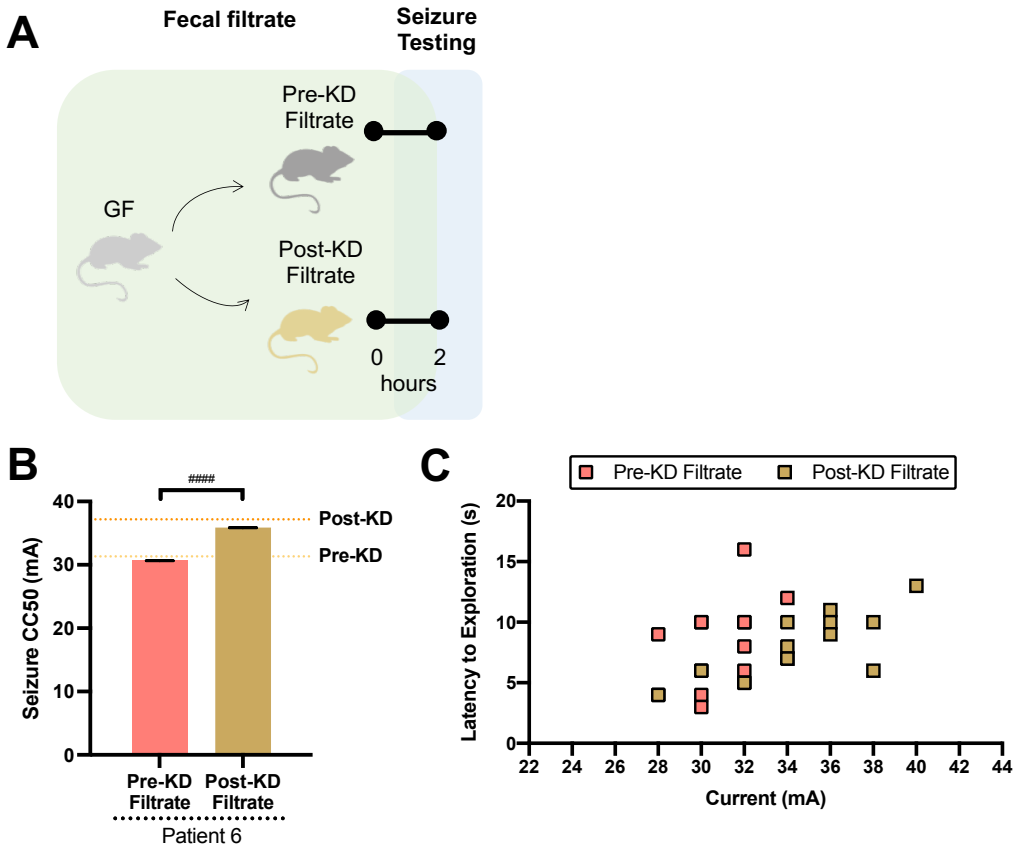

Figure S4: Small molecules from the clinical KD-associated human gut microbiome confer acute seizure protection, Related to Figure 1. **(A)** Experimental design for administration of human donor fecal filtrate samples to germ-free (GF) mice, followed by 6-Hz seizure testing 2 hours later. **(B)** Seizure thresholds for mice treated with sterile filtered pre-KD filtrate (n=13) and sterile filtered post-KD filtrate (n=14) fecal samples. Reference lines denote seizure thresholds for mice transplanted with unfiltered patient 6 post-KD and pre-KD relative control fecal microbiota from Figure 1B (One-way ANOVA with Tukey's, with # denoting statistical differences when considering within-patient recipient mice as technical replicates). **(C)** Latency to exploration for mice treated with sterile filtered pre-KD (n=13) and sterile filtered post-KD (n=14) that underwent 6-Hz psychomotor seizure testing. Data is displayed as mean ± SEM, unless otherwise noted. #### $p < 0.0001$ (for within-patient mouse recipients).

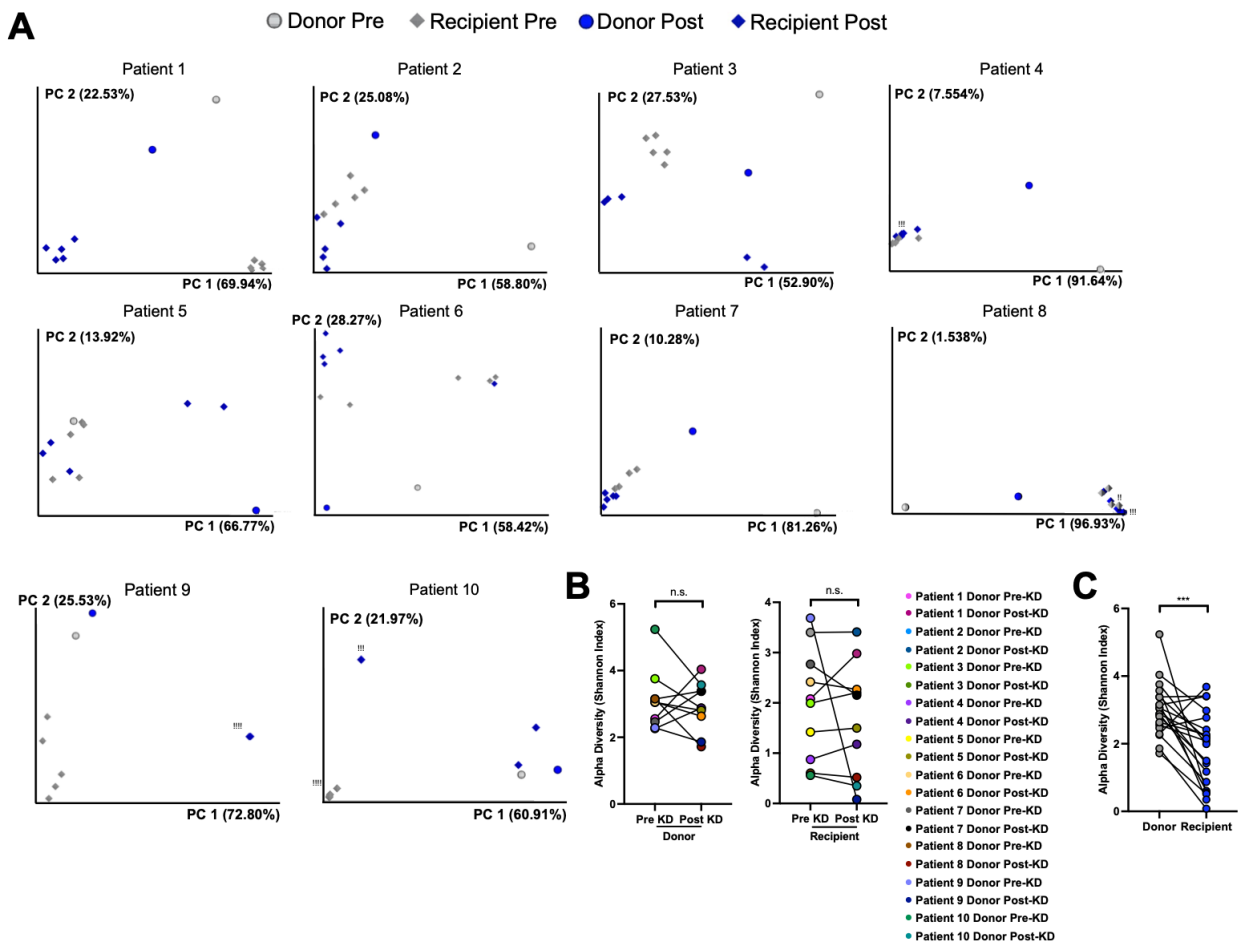

Figure S5: Taxonomic fidelity of human microbiota transfer to mice, Related to Figure 1. **(A)** Principal coordinates analysis of weighted UniFrac distances from 16S rRNA gene sequencing of fecal samples from matched human donors and mouse recipients (for each graph: n = 1 donor patient (10 patients total), 4-5 recipient cages of recipient mice per pre-KD vs. post-KD condition, ! = 1 overlapping data point not visible). **(B)** Shannon index alpha-diversity of fecal microbiota from human donor pre-KD and post-KD samples (left) and matched mouse recipient pre-KD and post-KD samples (right) (two-tailed, Wilcoxon matched-pairs signed rank test, donors: n=10 patients, recipients: n=10 per patient condition, where each n is an average from 4-5 cages per patient). **(C)** Shannon index alpha-diversity of fecal microbiota from all human donor samples (n=20 patients) and all matched mouse recipient samples (two-tailed, Wilcoxon matched-pairs signed rank test; n=20 patient conditions, where each n is an average from 4-5 cages per patient). Data is displayed as mean ± SEM, unless otherwise noted. ***$p < 0.001$, n.s.=not statistically significant.

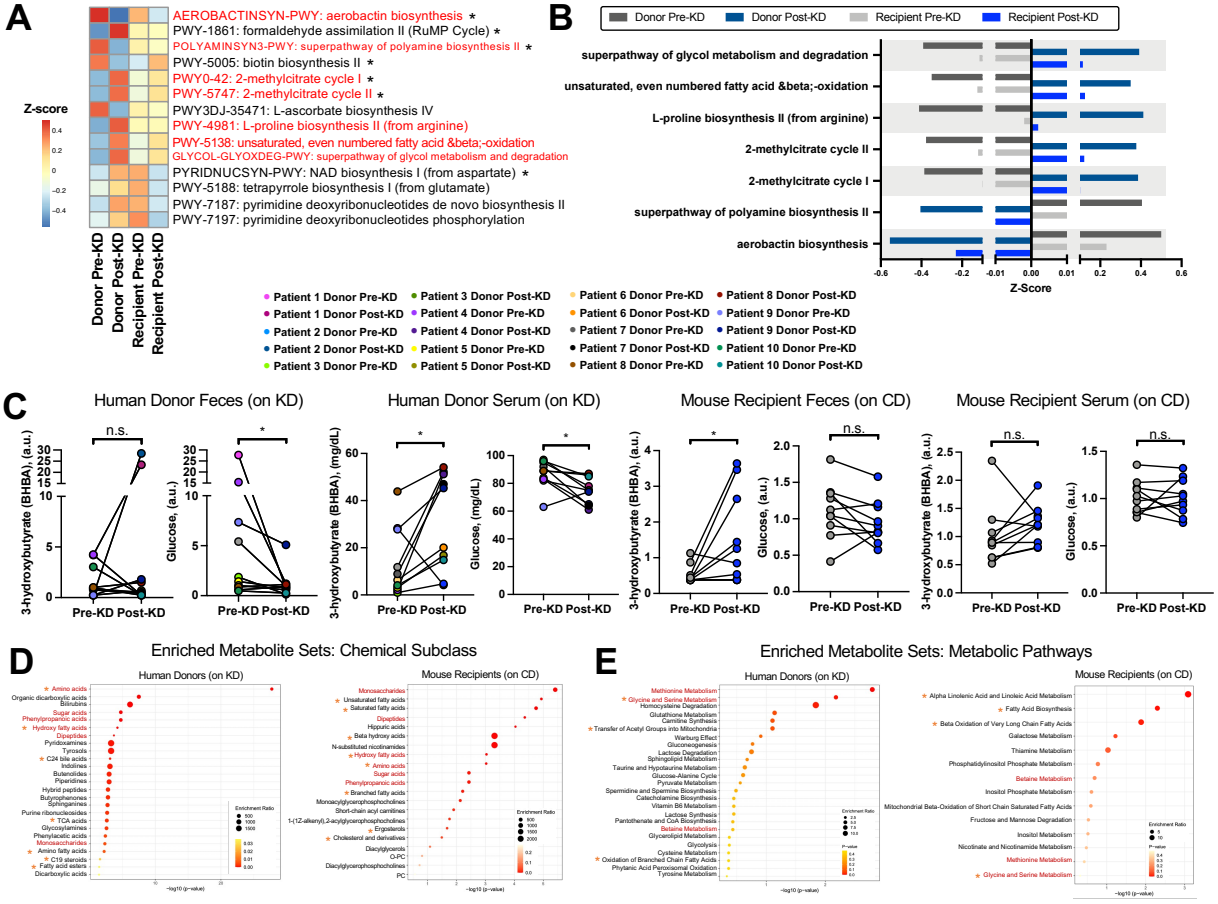

Figure 2: The clinical KD-associated human microbiome exhibits functional alterations that are phenocopied in seizure-protected recipient mice. **(A)** Microbial functional pathways differentially abundant as determined by MaAsLin2 analysis comparing post-KD (samples relative to pre-KD controls for either donor fecal samples or recipient fecal samples (donors: n=10 per diet condition; recipients: n=10 per donor diet condition [50 total, where each n reflects average of 5 technical replicate recipient mice per donor patient sample]). Red font denotes pathways that are commonly differentially abundant in the same direction in both donors fed KD and recipient mice fed CD (all pathways listed had minimum p<0.1; *denotes pathways with p<0.05). **(B)** Microbial functional pathways that are commonly differentially abundant by MaAsLin2 analysis in the same direction in post-KD donor and recipient controls (donors: n=10 per diet condition; recipients: n=10 per donor diet condition [50 total, where each n reflects average of 5 technical replicate recipient mice per donor patient sample]). **(C)** Beta-hydroxybutyrate (BHBA) and glucose levels in human donor (left) and mouse recipient (right) pre-KD and post-KD feces and serum (two-tailed Wilcoxon matched-pairs signed rank test; donors: n=10 per diet condition; recipients: n=10 per donor diet condition [50 total, where each n reflects average of 5 technical replicate recipient mice per donor patient sample]). **(D)** Metabolite set enrichment analysis showing the top 25 enriched chemical subclasses ordered by p-value for the set of differentially abundant metabolites in human donor (left) post-KD vs pre-KD fecal samples (p<0.05, two-tailed, matched pairs Student's t-test, n=10 per diet condition). Metabolite set enrichment analysis showing enriched chemical subclasses ordered by p-value for the set of differentially abundant metabolites in recipient mouse (right) post-KD vs pre-KD fecal samples (p<0.05, matched pairs Student's t-

test, n=10 per patient diet condition, where each sample is pooled from 5 recipient mice per donor patient sample). Red font denotes chemical subclasses altered in post-KD vs pre-KD human donor feces that are shared with those differentially regulated in post-KD vs pre-KD mouse recipient feces. Orange asterisks (*) denote additional chemical subclasses that are relevant to KD based on existing literature. **(E)** Metabolite set enrichment analysis showing the top 25 enriched SMPBD pathways by p-value for the set of differentially abundant metabolites in human donor (left) post-KD vs pre-KD fecal samples ($p<0.05$, matched pairs Student's t-test, n=10 per patient diet condition). Metabolite set enrichment analysis showing enriched SMPBD pathways by p-value for the set of differentially abundant metabolites in recipient mouse (right) post-KD vs pre-KD fecal samples ($p<0.05$, matched pairs Student's t-test; n=10 per patient diet condition, where each sample is pooled from 5 recipient mice per donor patient sample). Red font denotes metabolic pathways altered in post-KD vs pre-KD human donor feces that are shared with those differentially regulated in post-KD vs pre-KD mouse recipient feces. Orange asterisks (*) denote additional chemical subclasses that are relevant to KD based on existing literature. Data is displayed as mean ± SEM, unless otherwise noted. *$p < 0.05$. n.s.=not statistically significant. KD, ketogenic diet; BHBA, beta-hydroxybutyrate; CD, control diet; SMPDB, The Small Molecule Pathway Database; PC=phosphatidylcholine

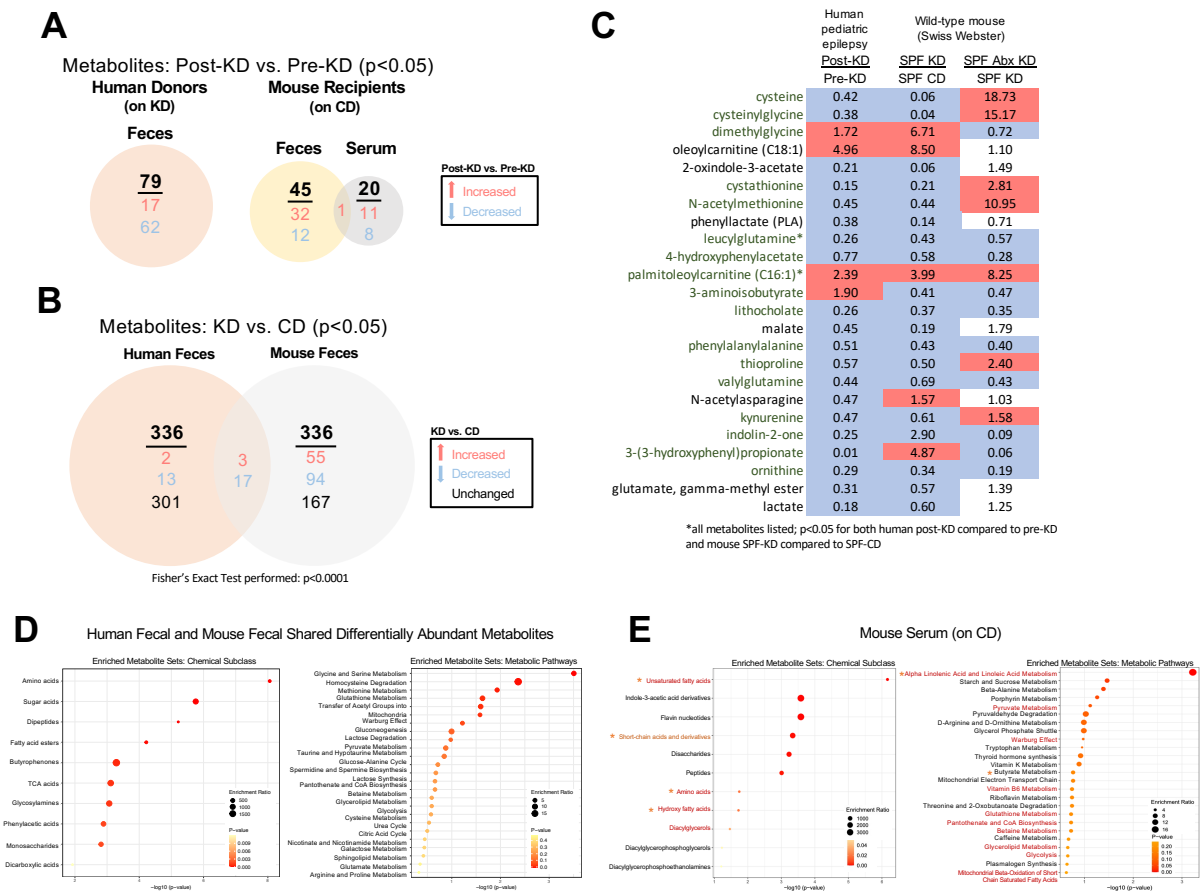

Figure S6: The clinical KD alters metabolomic profiles in human fecal samples and in fecal and serum samples of mice inoculated with human microbiota, Related to Figure 2. (A) Differentially abundant metabolites (p<0.05) in post-KD compared to pre-KD samples of human donor feces, mouse recipient feces, and mouse recipient blood (Two-tailed matched pairs Student's t-test, n=10 per condition, where each recipient sample is pooled from 5 recipient mice per donor patient sample) **(B)** Differentially abundant metabolites (p<0.05) in post-KD compared to pre-KD samples of human donor feces, which were also significantly altered in conventional mice (SPF) fed KD chow or vitamin- and mineral- matched control diet (CD) for 14 days. Red font denotes the subset of metabolites that were further altered by pre-treating KD chow-fed mice with antibiotics (Abx) to deplete gut bacteria. (human: Two-tailed matched pairs Student's t-test, n=10 per condition; mouse: ANOVA contrasts, n=8 per condition). **(C)** Differentially abundant metabolites (p<0.05) in human feces (post-KD compared to pre-KD) and feces of mice fed KD vs. CD chow for 14 days (Human fecal: Two-tailed matched pairs Student's t-test, n=10 per condition, where each recipient sample is pooled from 5 recipient mice per donor patient sample; Mouse fecal: two-way ANOVA with contrasts, n=8 per condition; Fisher's Exact Test). (**D**) Metabolite set enrichment analysis of chemical subclass for the 26 differentially abundant metabolites (p<0.05, matched pairs Student's t-test) found in both human post-KD vs pre-KD fecal samples and SFP mouse KD vs CD fecal samples (left) (human: n=10 per condition, where each sample is pooled from 5 recipient mice per donor patient sample; mouse: n=8 per condition). Metabolite set enrichment analysis of SMPDB pathways for the 26 differentially abundant metabolites (p<0.05, matched pairs Student's t-test) found in both human post-KD vs pre-KD fecal samples and SFP mouse KD vs CD fecal samples (right) (human: n=10 per condition, where each sample is pooled from 5 recipient mice per donor patient sample; mouse: n=8 per condition). **(E)** Metabolite set

enrichment analysis of chemical subclass for differentially abundant metabolites ($p<0.05$, matched pairs Student's t-test) in recipient mouse post-KD vs pre-KD serum samples (left) (n=10 per condition, where each sample is pooled from 5 recipient mice per donor patient sample). Metabolite set enrichment analysis of SMPDB pathways for differentially abundant metabolites ($p<0.05$, matched pairs Student's t-test) in recipient mouse post-KD vs pre-KD serum samples (right) (n=10 per condition, where each sample is pooled from 5 recipient mice per donor patient sample). Red font denotes metabolic pathways altered in post-KD vs pre-KD mouse serum that are shared with those differentially regulated in post-KD vs pre-KD mouse feces and/or human feces. Orange asterisks (*) denote additional chemical subclasses that are relevant to KD based on existing literature. KD, ketogenic diet; SPF, specific pathogen free conventionalized mice; CD, control diet; Abx, antibiotic SMPDB, The Small Molecule Pathway Database

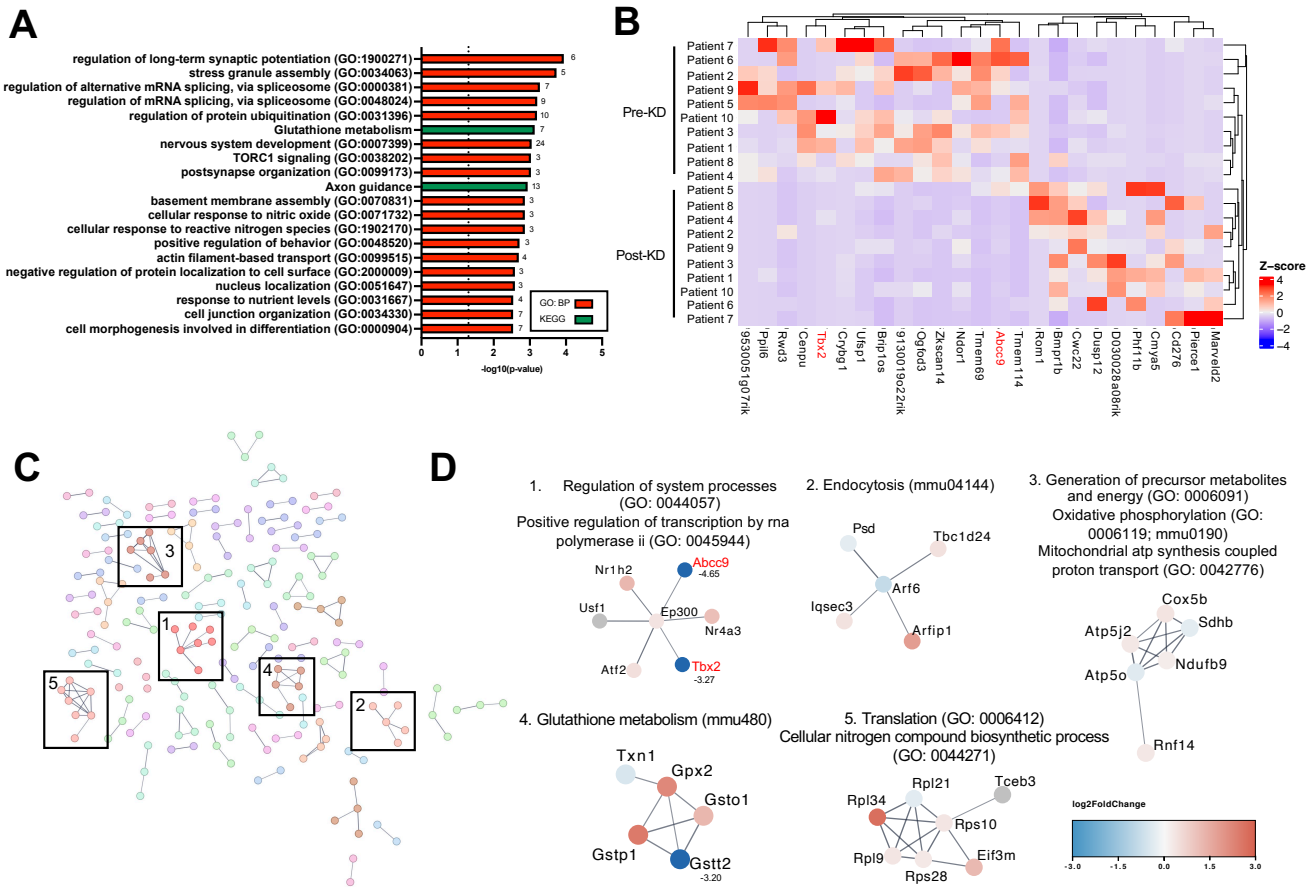

Figure 3: Seizure resistance in mice inoculated with the post-KD microbiota is associated with alterations in the brain transcriptome. **(A)** GO: Biological Process gene ontology of differentially expressed genes ($p<0.05$) in recipient mouse post-KD (n=10, where each sample is pooled from 6 recipient mice per donor patient sample) compared to pre-KD hippocampal samples, top 20 ranked by p-value (n=10 per patient diet condition, where each sample is pooled from 6 recipient mice per donor patient sample). **(B)** Heatmap of euclidian row and column clustered top 25 differentially expressed genes in recipient mouse post-KD compared to pre-KD hippocampus ranked by p-value, smallest to largest, and with log2 fold-change >2 (n=10 per patient diet condition, where each sample is pooled from 6 recipient mice per donor patient sample). **(C)** Protein interaction network with MCL clustering based upon mouse recipient post-KD and pre-KD hippocampal transcriptomics which appeared in both GO and STRING network enrichment analyses, STRING network enrichment score >0.7 (n=10 per patient diet condition, where each sample is pooled from 6 recipient mice per donor patient sample). **(D)** Functional enrichment of top MCL sub-network clusters from hippocampal transcriptomics STRING network analysis, proteins are colored based on their overall log2FC. If log2FC >3 or <-3, the value is listed next to the node name (n=10 per patient diet condition, where each sample is pooled from 6 recipient mice per donor patient sample). KD, ketogenic diet; GO, gene ontology; MCL, Markov Cluster Algorithm.

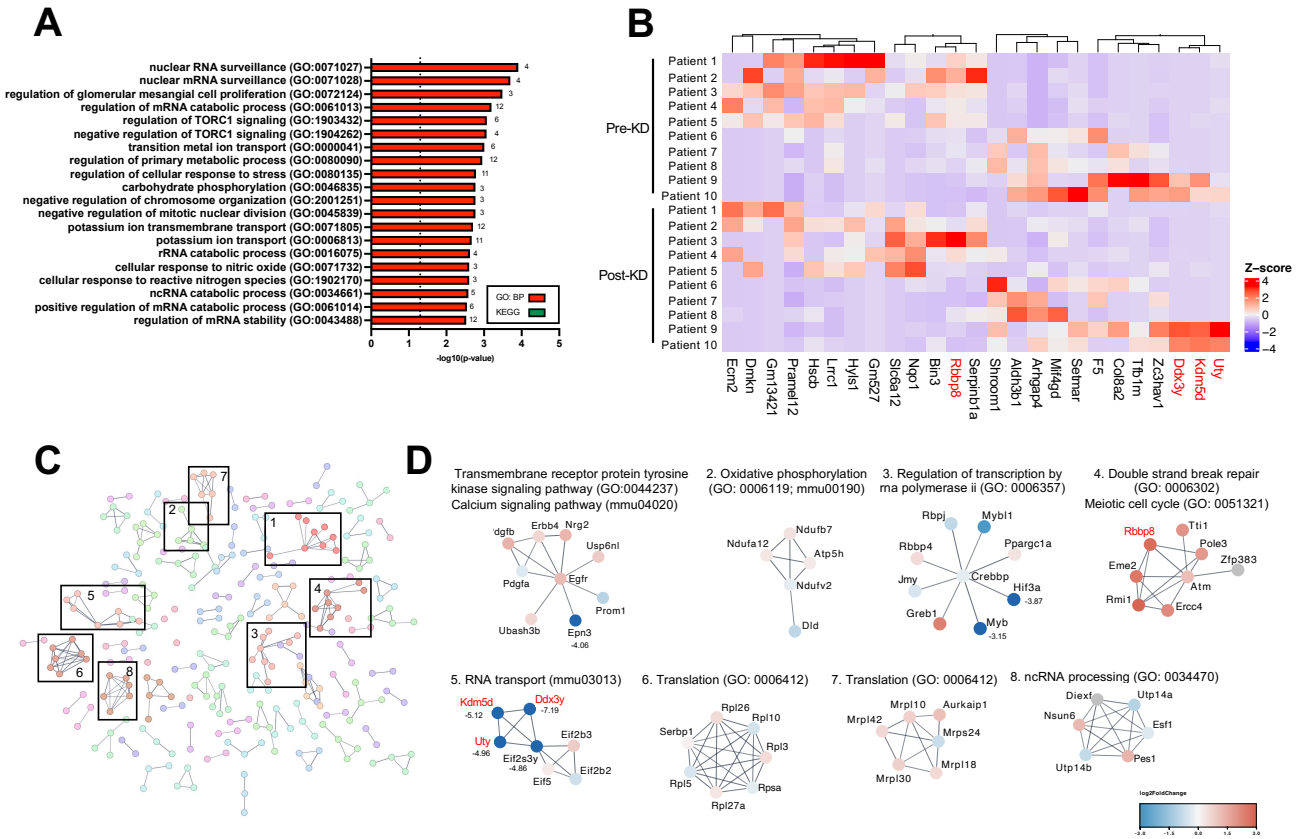

Figure S7: Mice inoculated with the post-KD microbiota exhibit alterations in the frontal cortical transcriptome, Related to Figure 3. **(A)** GO: Biological Process gene ontology of differentially expressed genes ($p<0.05$) in recipient mouse post-KD compared to pre-KD frontal cortex samples, top 20 ranked by p-value (n=10 per patient diet condition, where each sample is pooled from 6 recipient mice per donor patient sample). **(B)** Heatmap of top 25 differentially expressed genes in recipient mouse post-KD compared to pre-KD frontal cortex ranked by p-value, smallest to largest, with log2-fold change >2 (n=10 per patient diet condition, where each sample is pooled from 6 recipient mice per donor patient sample). **(C)** Protein interaction network with MCL clustering based upon mouse recipient post-KD and pre-KD frontal cortex transcriptomics which appeared in both GO and STRING network enrichment analyses, STRING network enrichment score >0.7 (n=10 per patient diet condition, where each sample is pooled from 6 recipient mice per donor patient sample). **(D)** Functional enrichment of top MCL sub-network clusters from frontal cortex transcriptomics STRING network analysis, proteins are colored based on their overall log2FC. If log2FC >3 or <-3, the value is listed next to the node name (n=10 per patient diet condition, where each sample is pooled from 6 recipient mice per donor patient sample). KD, ketogenic diet; GO, gene ontology; MCL, Markov Cluster Algorithm.

A

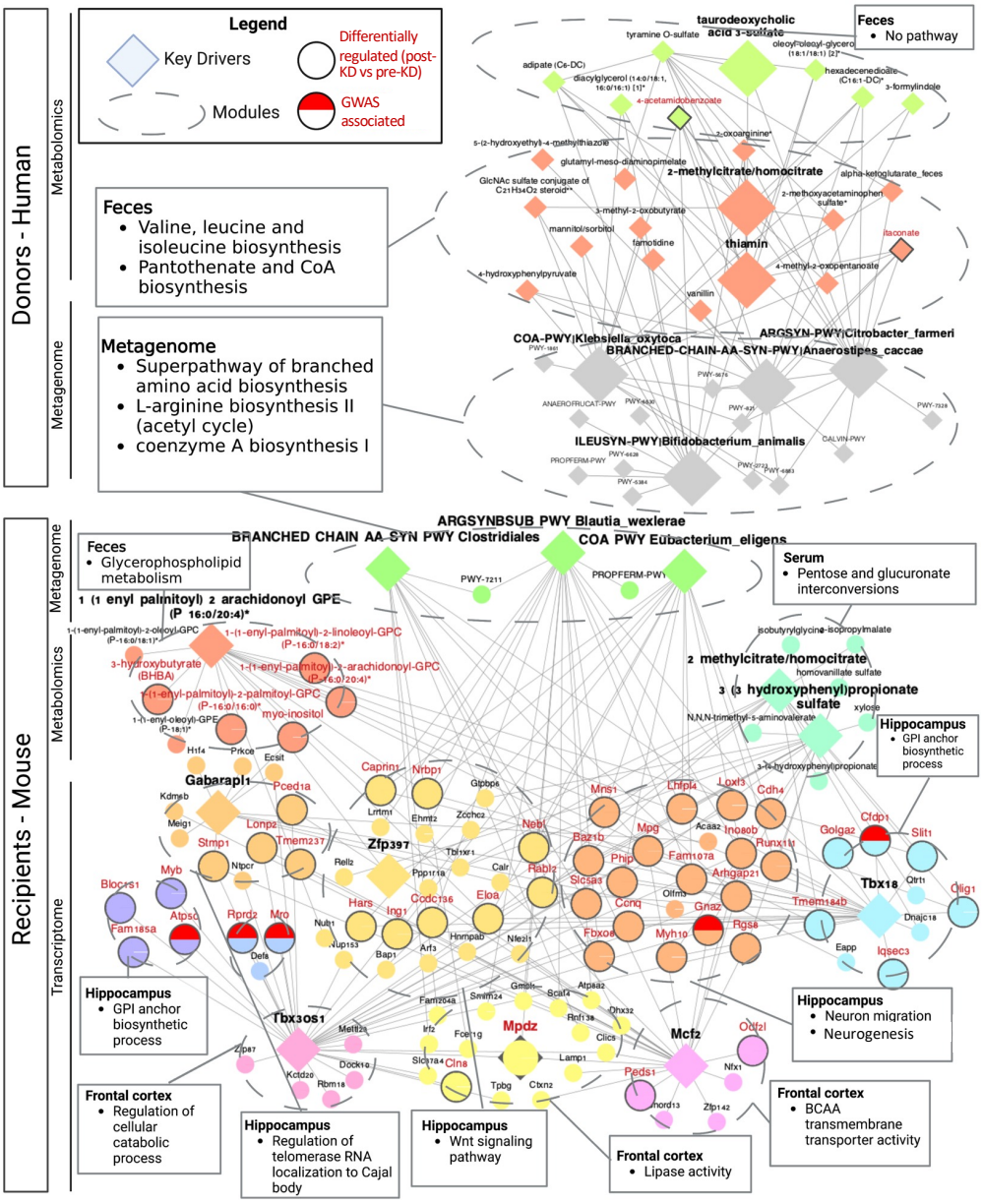

B

Brain Region	p-value	GWAS - Top Associated Genes
Hippocampus	0.003	RSAD1;JAM2;GAS5;TPPP;CYB561;METTL18;AP000350.5,GSTT2B,DDT,AP000351.4, MIF-AS1,AP000350.6,GSTT2;LRRC56,RNH1;ATXN2L,SULT1A1,SULT1A2,NPIPB7, NUPR1,EIF3C,SH2B1,TUFM;ATP23
Frontal cortex	0.26	RMI1;DLD;FLOT1,VARS2,CCHCR1;DPM2;EI24;SMIM19;S100A10;RANBP10,CARMIL2; RERE;NCKIPSD,WDR6

Figure 4: Multi'omic network analysis identifies key microbial genomic pathways and microbially modulated metabolites associated with differential expression of hippocampal transcripts. (A) MMVEC based co-occurrence network constructed from (top) human donor pre-KD and post-KD fecal metagenomic and fecal metabolomic datasets and (bottom) mouse recipient pre-KD and post-KD fecal metagenomic, fecal metabolomic, serum metabolomic,

hippocampal transcriptomic, and frontal cortical transcriptomic datasets. wKDA analyses was performed on the network. Red text denotes pathways, metabolites, or genes that were differentially regulated ($p<0.05$) between pre-KD and post-KD in prior individual dataset analyses (donor: n=10 patients per diet condition; recipient: n=10 per patient diet condition, where each sample is pooled from 5-6 recipient mice per donor patient sample). **(B)** Table of top associated genes from epilepsy GWAS mapping onto mouse recipient hippocampal and frontal cortical DEGs (n=10 per patient diet condition, where each sample is pooled from 6 recipient mice per donor patient sample). MMVEC, microbe-metabolite vectors; KD, ketogenic diet; wKDA, weighted key driver analysis; GWAS genome-wide association study; DEGs, differentially expressed genes